HHS Public Access

Author manuscript

Sci Transl Med. Author manuscript; available in PMC 2017 June 07.

Published in final edited form as:

Sci Transl Med. 2016 December 07; 8(368): 368ra173. doi:10.1126/scitranslmed.aah6571.

Five-coordinate H64Q neuroglobin as a ligand-trap antidote for carbon monoxide poisoning

Ivan Azarov[1,†], **Ling Wang**[1,2,†], **Jason J. Rose**[1,2,†], **Qinzi Xu**[1], **Xueyin N. Huang**[1], **Andrea Belanger**[5], **Ying Wang**[2], **Lanping Guo**[2], **Chen Liu**[5], **Kamil B. Ucer**[5], **Charles F. McTiernan**[1,2], **Christopher P. O'Donnell**[1,2], **Sruti Shiva**[1,3,4], **Jesús Tejero**[1,2], **Daniel B. Kim-Shapiro**[5,6], and **Mark T. Gladwin**[1,2,*]

[1]Pittsburgh Heart, Lung, Blood and Vascular Medicine Institute, University of Pittsburgh, Pittsburgh, Pennsylvania, USA 15261

[2]Division of Pulmonary, Allergy and Critical Care Medicine, UPMC and University of Pittsburgh, Pittsburgh, Pennsylvania, USA 15261

[3]Department of Pharmacology and Chemical Biology, University of Pittsburgh, Pittsburgh, Pennsylvania, USA 15261

[4]Center for Metabolism and Mitochondrial Medicine (C3M), University of Pittsburgh, Pittsburgh, Pennsylvania, USA 15261

[5]Department of Physics, Wake Forest University, Winston-Salem, North Carolina, USA 27109

[6]Translational Science Center Wake Forest University, Winston-Salem, North Carolina, USA 27109

Abstract

Carbon monoxide (CO) is a leading cause of poisoning deaths worldwide, with no available antidotal therapy. We introduce a potential treatment paradigm for CO poisoning, based on near-irreversible binding of CO by an engineered human neuroglobin (Ngb). Ngb is a six-coordinate hemoprotein, with the heme iron coordinated by two histidine residues. We mutated the distal histidine to glutamine (H64Q) and substituted three surface cysteines with less reactive amino acids to form a five-coordinate heme protein (Ngb-H64Q-CCC). This molecule exhibited an

*Corresponding author. gladwinmt@upmc.edu.
†These authors contributed equally to this work.

Author contributions: M.T.G. conceived and supervised the project. I.A. designed and performed most *in vitro* experiments and some *in vivo* experiments. L.W. designed and performed most *in vivo* experiments. J.J.R. and S.S. designed and performed some *in vitro* experiments. Q.X. performed the ventilated animal experiments. J.T. designed the H64Q-CCC modified neuroglobin, aided in expression and production and conducted some *in vitro* experiments. X.N.Y. performed the protein expression and purification. Y.W. and L.G. conducted animal surgery. C.P.O. and C.F.M. assisted with experimental design and critical review of the manuscript. A.B., C.L., and K.B.U. conducted laser photolysis and time resolved absorption experiments. D.B.K-S. designed and supervised laser photolysis and time resolved absorption experiments. All authors wrote and edited parts of the manuscript, read and approved the final manuscript.

Competing interests: M.T.G. and J.T. have submitted a provisional patent filing on the use of recombinant neuroglobin mutants for carbon monoxide poisoning. The other authors declare that they have no competing interests. Data and Materials Availability: Raw data and materials are available from the authors for noncommercial researchers via a materials transfer agreement.

SUPPLEMENTARY MATERIALS
Methods
References: (68–71)

unusually high affinity for gaseous ligands, with a P_{50} value for oxygen of 0.015 mmHg. Ngb-H64Q-CCC bound CO about 500 times more strongly than did hemoglobin. Incubation of Ngb-H64Q-CCC with 100% CO-saturated hemoglobin, either cell-free or encapsulated in human red blood cells, reduced the half-life of carboxy-hemoglobin to 0.11 and 0.41 minutes, respectively, from a value that is ≥ 200 minutes when the hemoglobin or cells are only exposed to air. Infusions of Ngb-H64Q-CCC to CO-poisoned mice enhanced CO removal from red blood cells, restored heart rate and blood pressure, increased survival, and were followed by rapid renal elimination of CO-bound Ngb-H64Q-CCC. Heme-based scavenger molecules with very high CO binding affinity such as our mutant five-coordinate Ngb are potential antidotes for CO poisoning by virtue of their ability to bind and eliminate CO.

INTRODUCTION

Carbon monoxide (CO) poisoning results in an estimated 50,000 emergency department visits in the United States annually and is one of the leading causes of poisoning death globally (1). Despite the fact that it has been appreciated since the 19th century that CO produces tissue hypoxia by binding avidly to hemoglobin (Hb) (2, 3), to date there is no approved specific antidotal therapy. Beyond the provision of supplemental normobaric and hyperbaric oxygen, treatment has not changed significantly over the last several decades (1, 4). Patients with severe CO poisoning exhibit lactic acidosis, hemodynamic instability, and respiratory failure, which often limit their access to hyperbaric therapy. Although hyperbaric oxygen therapy reduces neurological impairment resulting from CO poisoning, substantive deficits usually remain (1, 5, 6). New and effective approaches are urgently needed to treat CO poisoning (7).

Neuroglobin (Ngb) is a cellular hemoprotein expressed in brain and retina that protects cells from death after ischemia and reperfusion injury (8–10). Mechanisms proposed for this cytoprotective effect include the reduction of cytochrome c or the reduction of nitrite to form nitric oxide (NO) (11–13). Unlike five-coordinate globins such as Hb and myoglobin (Mb), wild type Ngb has a distal histidine residue (H64) that binds to the heme iron, resulting in a six-coordinate heme (14). This bis-histidine structure is common to cytochromes and other globins (cytoglobin (15), plant Hbs (16), drosophila Hb (17)). In an effort to understand the mechanisms that regulate nitrite and other ligand binding to Ngb, we generated H64 mutants that are constitutively five-coordinate (free iron ligand position similar to Hb and Mb) (Fig. 1A) (12, 18). These five-coordinate mutant Ngb molecules can reduce nitrite to form NO about 2,500 times faster than Hb (12, 18), bind oxygen with very high affinity (P_{50} ≈ 0.015 mmHg, Fig. S1) and show even higher affinities for CO (14, 19).

The essential properties of a CO scavenger, particularly under aerobic conditions, are: (i) high CO association rate (k_{on}) and equilibrium association constants (K_A), relative to Hb; (ii) high M-value (K_A CO/K_A O_2) to allow CO scavenging in oxygenated blood; and (iii) a low rate of autoxidation (k_{autox}) to allow maintenance of the reduced ferrous state, required for ligand binding. An oxygen-bound hemoprotein with a high M-value has the added advantage of releasing an oxygen molecule while binding CO. We propose that mutant five-

coordinate Ngb could satisfy these requirements and serve as a CO scavenger for the treatment of CO poisoning by binding and eliminating CO.

RESULTS

H64 substituted Ngb exhibits a higher CO binding affinity than Hb

Previous studies have identified proteins with notably high affinities for CO. For example, the Hb from *Glycera dibranchiata* has a very high association constant for CO ($K_A = 6.4 \times 10^8\ M^{-1}$) (20) when compared to the value for sperm whale Mb ($K_A = 2.7 \times 10^7\ M^{-1}$; Table S1) (21). In *Glycera dibranchiata* Hb, the distal histidine residue is replaced by a leucine; the introduction of the same replacement in Mb substantially increases the affinity for CO ($K_A = 1.1 \times 10^8\ M^{-1}$) (21). However, these high CO affinities are still below the value of the high affinity R-state Hb ($K_A = 6.0 \times 10^8\ M^{-1}$) (22), suggesting that they would not scavenge CO effectively from CO-saturated hemoglobin. Our group has studied the effects of a similar substitution of the distal histidine of Ngb on nitrite reduction and other heme properties (12, 18). During the purification of these Ngb His64 mutants, we and others have detected the presence of NO (or CO) bound-Ngb (18, 23). This observation, together with the high CO binding rates of wild type and H64L neuroglobins (14, 19), suggested that distal histidine mutants of Ngb might have very high affinities towards CO and could function as CO-scavenging molecules. Such a molecule has the potential to bind oxygen and CO, and if the CO affinity is higher than oxygen affinity (a high M-value), the molecule would scavenge CO and release oxygen. As previous studies indicate that H64Q Ngb shows a lower autoxidation rate than most Ngb mutants and could more stably bind oxygen (18), we focused on this mutant as a possible CO-scavenging molecule.

We measured CO binding affinities in recombinant Ngb molecules and Hb at room temperature (22 °C) using laser flash photolysis to assess on-rates and NO displacement of CO for analysis of off-rates (Fig. 1B). Two Ngb mutants were evaluated: H64Q (Ngb-H64Q) and H64Q combined with three surface thiol substitutions (C46G/C55S/C120S; Ngb-H64Q-CCC) to increase protein solubility and limit oligomerization at high protein concentrations. The flash photolysis methodology allows for full release of CO from the heme and fast measurement of CO rebinding. To analyze the species formed during the reaction, we used standard reference spectra. Static absorption spectra, normalized by concentration to produce millimolar extinction coefficients, are shown for deoxy- and CO-Ngb-H64Q-CCC in Fig. 1C. The difference between these two spectra is shown in Fig. 1D. To measure CO association rate constants, the CO-bound globins were photolysed with a 20 mJ, 6 ns Nd-YAG laser pulse at 532 nm, and the recombination kinetics were recorded for 1200 μs and 100 μs for Hb and Ngbs, respectively. The absorption difference spectra were calculated as the absorbance at a time t minus the absorption prior to photolysis. Upon photolysis, the absorption difference spectrum is expected to be similar to that shown in Fig. 1D (deoxy minus CO-bound). As CO rebinds, the difference spectrum is expected to go to zero as the final state becomes identical to the initial CO-Ngb state. The resulting absorption difference spectra were fit to first order kinetics by using global analysis with SpecFit software (24). The two forms of Ngb (Ngb-H64Q and Ngb-H64Q-CCC) had similar association rate constants for CO, which were much faster than Hb. Fig. 1E shows initial and final

absorption difference spectra of Hb 1200 μs after the 20 mJ laser pulse and of Ngb 100 μs after the pulse, reflecting the time it takes to rebind CO after flash photolysis. Note that the Hb reaction with CO is still incomplete after 1000 μs, with Hb not yet 100% bound by CO (Fig. 1E, F). The absorbance difference changes for the 440 nm peak illustrate the difference in association rates; the time decay and first order fit of the absorbance difference are shown in Fig. 1F on a logarithmic scale. We monitored the binding around 440 nm because as the spectral changes are more pronounced and the sensitivity of the measurements is better at this wavelength, allowing the use of less protein and a laser pulse of minimal energy (but that still produced a measurable photolysis yield). Both Ngb molecules bound CO faster than did Hb with calculated bimolecular association rate constants of $1.3 \pm 0.4 \times 10^8$ $M^{-1}s^{-1}$ and $1.6 \pm 0.4 \times 10^8$ $M^{-1}s^{-1}$ for Ngb-H64Q and Ngb-H64Q-CCC, respectively, and $5.0 \pm 1.4 \times 10^6$ $M^{-1}s^{-1}$ for Hb.

To determine the dissociation rates of CO from the Ngb mutants, the kinetics of CO displacement by NO were followed spectroscopically after mixing CO-bound globins with a solution containing a high concentration of NO. As NO is present in large excess (1 mM NO vs. 10 μM CO) and binds to Ngb with very high affinity (14), released CO molecules are quickly replaced by NO (25). Samples of 10 μM CO-bound protein containing 100 μM sodium dithionite were mixed with 1mM NO and immediately scanned. Absorption spectra were recorded for 45 minutes for Hb and 270 minutes for Ngb (Fig. 1G and H). As the spectral changes for the two mutant Ngb molecules are similar, only Ngb-H64Q-CCC is shown. The measured dissociation rate constants were $5.2 \pm 1.4 \times 10^{-4}$ s^{-1} and $4.2 \pm 1.8 \times 10^{-4}$ s^{-1} for Ngb-H64Q and Ngb-H64Q-CCC, respectively, and $6.5 \pm 2.0 \times 10^{-3}$ s^{-1} for Hb. The overall measured affinities ($K_A = k_{on}/k_{off}$ values shown in Fig. 1I) were 7.95×10^8 M^{-1} for Hb compared with $2.54 \pm 1.13 \times 10^{11}$ M^{-1} and $3.80 \pm 0.96 \times 10^{11}$ M^{-1} for Ngb-H64Q and Ngb-H64Q-CCC, respectively. When compared to our determined values for Hb, Ngb-H64Q and Ngb-H64Q-CCC exhibited 319- and 478-fold greater affinities for CO, respectively (Fig. 1I).

Because oxygen and CO are both present in blood, a CO scavenger molecule must have a high M-value (K_A CO/K_A O_2) to be able to scavenge CO in competition with blood oxygen. An oxygenated hemoprotein with a high M-value would also release oxygen as it binds CO. To determine the relative affinity of Ngb-H64Q-CCC towards oxygen, we determined the association and dissociation rates for the reaction of Ngb-H64Q-CCC and oxygen. CO-Ngb-H64Q-CCC (20 μM) in buffer containing 100 μM CO and 225 μM oxygen was photolyzed and the replacement by oxygen was monitored for 30 μs after photolysis. The absorption difference spectra (transient – ground state) were calculated and fit by using single value decomposition and global analysis to a single exponential decay (similar approach as described above for CO rebinding). The observed rate constant for these data obtained from the fit was 0.12 μs^{-1}. The bimolecular rate constant for oxygen binding was $7.2 \pm 1.5 \times 10^8$ $M^{-1}s^{-1}$ (Fig. S2).

In order to determine the dissociation rate of oxygen from Ngb-H64Q-CCC, we used the CO replacement method (see Methods). In short, freshly prepared oxy-Ngb complex (to avoid substantial presence of met-Ngb) was mixed with different concentrations of CO and the rate of decay of the oxy-Ngb complex (identical to the rate of formation of the CO-Ngb

complex) was measured. The observed rates increase hyperbolically as the [CO]/[O_2] ratio increases, with the oxygen dissociation rate being the limiting rate as [CO]/[O_2] becomes larger. We determined a rate for the reaction of 18.4 ± 0.7 s^{-1} (Fig. S2).

The measured oxygen association and dissociation rates indicate that the oxygen equilibrium association constant ($K_A = k_{on}/k_{off}$) is 3.9×10^7 M^{-1}, lower than the CO association constant (3.8×10^{11} M^{-1}). The M value is 9.7×10^3, suggesting that Ngb-H64Q-CCC would preferentially bind CO in the presence of mixtures of CO and oxygen.

To further characterize the properties of Ngb-H64Q-CCC, we determined the autoxidation and nitrite reduction rates of the mutant at 37°C, as described in Supplementary Materials. We observed autoxidation rates of 0.86 ± 0.33 h^{-1} (Fig. S3) similar to the reported value for the Ngb-H64Q mutant (0.60 ± 0.12 h^{-1}) (18). The nitrite reduction rate constant was 320 ± 10 $M^{-1}s^{-1}$ (Fig. S4), also in agreement with the rate for the Ngb-H64Q mutant (390 ± 20 $M^{-1}s^{-1}$) (18); both rates were 2,500 times faster than those for human hemoglobin A (T-state values (12, 26)). We also performed CO flash photolysis binding studies at lower CO concentrations to exclude potential artifacts of geminate recombination, as described in the Methods section of Supplementary Materials.

Compared to other heme-containing molecules, the Ngb-H64Q mutation confers the highest CO affinity (Table 1), three orders of magnitude higher than Hb. The Ngb-H64Q-CCC mutant also has a high M value. Finally, the autoxidation rate of Ngb-H64Q-CCC is slower than that of other hemoproteins with high CO affinity, supporting the ability of Ngb-H64Q-CCC to work as a rapid CO scavenger in vivo.

In vitro rapid CO transfer from carboxy-hemoglobin to Ngb-H64Q-CCC

We next evaluated the CO transfer from carboxy-Hb (CO-Hb) to Ngb-H64Q-CCC at 37°C under anaerobic (Fig. 2A–C) and aerobic (Fig. 2D–F) conditions (21% O_2, 1 atm). Under anaerobic conditions, 100% CO-Hb was rapidly mixed with equimolar solutions of deoxy Ngb-H64Q-CCC. We calculated the half-lives of CO dissociation from free Hb in the presence of Ngb-H64Q-CCC via single exponential fits. The experiments with free Hb were performed by using rapid manual mixing (time < 5 s) in a Cary spectrophotometer. Spectral deconvolution of time-resolved absorption data collected at 37°C was accomplished by a least squares fit with reference spectra (Fig. S5) to determine the percentage of: CO-Ngb, CO-Hb, deoxy-Ngb, deoxy-Hb, oxy-Ngb and oxy-Hb (12, 27–30). Fig. 2A shows the absorbance spectra of CO-Hb and deoxy-Ngb-H64Q-CCC before mixing and Fig. 2B shows absorbance spectra measured every 2.4 s after the two proteins were mixed under anaerobic conditions. As shown in Fig. 2C, after mixing, CO rapidly transferred from Hb to Ngb-H64Q-CCC, and the reaction was completed in approximately 30s. Fig. 2D–F shows similar experiments under aerobic conditions. Consistent with the measured higher affinity of Ngb-H64Q-CCC for CO compared with oxygen, there was minimal difference between the rates of CO transfer under anaerobic and aerobic conditions, with an average half-life (n = 7) of 6.4 ± 1.8 s based on single exponential fits.

We compared the dissociation rate of CO-Hb in the presence of excess Ngb-H64Q-CCC under anaerobic conditions to the dissociation rate of CO-Hb in the presence of 1 mM NO at

22 °C. The CO dissociation rate constants with Ngb-H64Q-CCC were 2.4 times faster than the rates measured in presence of excess NO ($0.014 \pm 0.005\ s^{-1}$ vs. $0.0065 \pm 0.002\ s^{-1}$) (Fig. S6). This difference may result from the fact that during Hb-CO dissociation measured by NO displacement Hb is in the R state throughout the reaction, because binding of both CO and NO to Hb stabilizes the R-state. When CO dissociates from Hb in the presence of Ngb-H64Q-CCC, the Hb is initially in the R state and then transitions to the deoxygenated T-state as the CO is released from Hb. As the CO dissociation rate for T-state Hb is about 10 times faster than for the R-state (Table 1), Ngb-H64Q-CCC can scavenge CO from CO-Hb faster than the dissociation of CO from R-state Hb in the presence of NO.

Rapid CO transfer from 100% CO saturated RBCs to extracellular Ngb-H64Q-CCC

We next tested how fast CO transfers from free Hb to Ngb-H64Q-CCC across cellular compartments, from the red blood cell (RBC) to extracellular Ngb. To evaluate this we prepared 100% CO-saturated RBCs and incubated them at 37 °C with different ratios of extracellular Ngb-H64Q-CCC to intracellular CO-Hb under anaerobic (Fig. 3A–D) and aerobic (Fig. 3E, F) conditions. After mixing, we determined the values at frequent time points by centrifuging samples in <5 s to separate erythrocytes from Ngb and measured CO bound to the intracellular Hb and to the supernatant Ngb-H64Q-CCC. The changes in absorbance spectra of Hb and Ngb-H64Q-CCC from a representative anaerobic experiment at 37 °C are shown in Fig. 3A and Fig. 3B, respectively. The Hb spectra changed from 100% CO-Hb to deoxy-Hb within 2 minutes, while the Ngb-H64Q-CCC spectra showed a complementary change of 100% deoxy-Ngb to CO-Ngb at the same time. Fig. 3C–F show example kinetics of the decrease in CO-Hb and increase in CO-Ngb-H64Q-CCC at different stoichiometric ratios of Ngb to Hb under anaerobic and aerobic conditions. The CO-Hb decay was fitted to a single exponential equation. The average rate constants for the reaction were $1.69 \pm 0.21\ min^{-1}$ ($0.028 \pm 0.004\ s^{-1}$) for combined anaerobic and aerobic experiments (CO-Hb half-life = 0.41 min); $1.92 \pm 0.31\ min^{-1}$ for anaerobic only; $1.25 \pm 0.12\ min^{-1}$ for aerobic only. When atmospheric oxygen was present (Fig. 3E, F), we observed a reduction in the magnitude of CO transfer from Hb to Ngb, although we did not see a statistically significant difference in the rate of CO removal from CO-Hb compared to that in the absence of oxygen. The decrease in the total amount of CO scavenged is likely due to the partial oxidation of the oxy-Ngb-H64Q-CCC to form the met-Ngb-H64Q-CCC species, which cannot bind CO. The analysis of all experiments, including those with free, unencapsulated Hb, indicated a 1:1 stoichiometric transfer of CO from Hb to Ngb-H64Q-CCC under both aerobic and anaerobic conditions (Fig. 3G).

The lack of an effect of oxygen on the rates of CO scavenging seems counterintuitive, as Ngb-H64Q-CCC has a high association rate constant for oxygen (Table 1). To further investigate these results, we used a mathematical approximation to the observed rates at half-reaction for equimolar initial amounts of CO-Hb and Ngb. The observed rates of CO scavenging in the absence (Equation 1) or the presence of oxygen (Equation 2) can be described as:

$$r_{obs,\,50\%} \approx \frac{k_{off\ CO,Hb}}{1+\frac{k_{on\ CO,Hb}}{k_{on\ CO,Ngb}}} \quad \text{(Equation 1)}$$

$$r_{obs,\,50\%} \approx \frac{k_{off\ CO,Hb}}{1+\frac{k_{on\ CO,Hb}\times P_{50,HbO_2}}{k_{on\ CO,Ngb}\times P_{50,NgbO_2}}} \quad \text{(Equation 2)}$$

Where k_{on} and k_{off} denote the binding and dissociation rates for the ligands and proteins indicated. The P_{50} values can be approximated by the dissociation rates divided by the association rates, so $P_{50,HbO2} \approx k_{off\ O2,Hb}/k_{on\ O2,Hb}$ and $P_{50,NgbO2} \approx k_{off\ O2,Ngb}/k_{on\ O2,Ngb}$. A detailed derivation of these expressions is provided in the Methods section of Supplementary Materials.

Substituting the experimental values (Table 1) into equations 1 and 2, we find that the high association rate constant of Ngb-H64Q-CCC towards CO makes the $k_{on\ CO,Hb}/k_{on\ CO,Ngb}$ term small, and thus the calculated observed rates correspond to $r_{obs} \approx 0.96 \times k_{off\ CO,Hb}$ in anaerobic conditions. However, in aerobic conditions the affinity towards oxygen is higher for Ngb-H64Q-CCC than for Hb, and this partly offsets the CO-dependent portion of the term, with $(k_{on\ CO,Hb} \times P_{50,HbO2})/(k_{on\ CO,Ngb} \times P_{50,NgbO2}) = 0.43$ and thus $r_{obs} \approx 0.70 \times k_{off\ CO,Hb}$. This small effect of oxygen on the observed rates is in very good agreement with our experimental data. Computer simulations using the experimental rate constants (see Supplementary Materials for details) suggest even smaller differences, with $r_{obs} \approx 1.04 \times k_{off\ CO,Hb}$ in anaerobic conditions and $r_{obs} \approx 0.90 \times k_{off\ CO,Hb}$ in aerobic conditions. These results can be understood by observing that the effect of oxygen in decreasing the amount of deoxyNgb available for CO scavenging is offset by the decrease in deoxyHb, which can rebind free CO and slow the reaction.

To better characterize the CO removal efficacy of Ngb-H64Q-CCC, wild type Ngb, apoNgb, albumin (BSA), and oxidized Ngb (met-Ngb) were tested as additional controls. Wild type Ngb incubated with CO-saturated RBCs bound CO at a significant slower rate ($k_{obs} = 0.61 \pm 0.15\ min^{-1}$; CO-Hb half-life 1.3 min) than did the mutant five-coordinate molecule, while other molecules did not bind CO at all and did not affect CO removal from CO-saturated RBCs (Fig. 3H). Half-lives of CO dissociation from RBC-encapsulated or free Hb from mouse and humans are summarized in Fig. 3I. When only atmospheric oxygen was available to displace CO from the Hb in human RBCs, the observed CO-Hb half-life was > 500 minutes, while in the presence of Ngb-H64Q-CCC, with and without atmospheric oxygen, it was reduced to only 0.41 minutes (25 s) (Fig. 3I). The CO-Hb half-life was about 0.11 minutes (7s) with mixtures of free CO-Hb and Ngb-H64Q-CCC. The difference in CO scavenging rates by Ngb-H64Q-CCC from RBC vs. free Hb (0.41 vs. 0.11 min half-life) yielded a quantitative estimation for the effect of the diffusion barrier to CO movement out of the cells, a result of slow diffusion in the highly viscous red cell cytoplasm and unstirred

layers external to the cell. In both cases, the rates in the presence of Ngb-H64Q-CCC were orders of magnitude faster than the corresponding rates in the absence of a scavenging agent.

In the presence of air, CO dissociation from purified free Hb (222 minutes half-life) was more than twice as fast as the release from RBC-encapsulated Hb (> 500 minutes half-life), indicating the very slow CO release in more physiological conditions. (Fig. 3I).

Ngb-H64Q-CCC rapidly removes CO from Hb in a non-lethal, CO poisoning mouse model

To test whether Ngb-H64Q-CCC can effectively remove CO *in vivo,* we exposed mice to 1,500 ppm CO gas mixed with air (Fig. 4), which steadily increased systemic CO-Hb levels, plateauing at 64 ± 1% (n = 13, PBS- & Ngb-infused mice combined) after 50 minutes of CO exposure. No animals died with this concentration and duration of CO exposure. We then stopped CO exposure and infused 250 μL of 9 – 12 mM Ngb-H64Q-CCC (either deoxy or partially oxy, see Table S1) or a similar volume of PBS over 4 minutes. Immediately after the infusion and every 5 minutes, 5 μl of blood was collected and the RBCs were rapidly washed and lysed for the measurement of CO-Hb. In contrast to PBS, the Ngb-H64Q-CCC rapidly cleared CO from RBCs in vivo (Fig. 4A), and CO clearance was associated with increases in arterial blood pressure (Fig. 4B). Fig. 4C, D show representative absorbance spectra of Hb from the blood of a CO-poisoned mouse that received an infusion of PBS (Fig. 4C) and from a mouse that received an infusion of Ngb-H64Q-CCC (Fig. 4D). The first absorbance spectrum shown (0 min) was taken at the time when CO-exposure was stopped and the animals were returned to normal atmospheric conditions. These spectra indicate 58% and 57% CO-Hb, respectively, for the mice with PBS and Ngb-H64Q-CCC infusions. The subsequent spectra for both animals were recorded every 5 min for 30 min, followed by spectra at two 10-min intervals. The mouse receiving Ngb-H64Q-CCC had a much lower CO-Hb% after the first 5 minutes than the mouse that received PBS (Fig. 4C, D). Five minutes after return to normal atmospheric conditions, which is at least 30 s after the end of infusions, the CO-Hb levels dropped by an average of 35.0 ± 2.1% in the group that received Ngb-H64Q-CCC (n = 6) but only 13.3 ± 0.6% in the group that received PBS (n = 7) (Fig. 4E). The decrease in blood pressure during CO exposure was similarly low in the two groups (Fig. 4B) and consistent with severe hemodynamic instability during CO poisoning. At the end of the exposure, blood pressure in mice that received Ngb-H64Q-CCC was restored to near its pre-exposure values in contrast to the lower blood pressures of animals that received PBS ($P = 0.0006$ for time > 0, using a mixed effect model with unstructured covariance, Fig. 4B). This effect may be partly a result of rapid CO clearance, although a contribution from NO scavenging by Ngb-H64Q-CCC due to the high initial amounts of the oxy Ngb-H64Q-CCC cannot be excluded. Sixty minutes after infusion, we unexpectedly detected high concentrations of Ngb (86 – 94% CO-Ngb) in the bladder, indicating the rapid removal of CO by Ngb-H64Q-CCC and rapid clearance of CO-Ngb-H64Q-CCC from blood to urine (Fig. 4F). In these studies, we evaluated Ngb-H64Q-CCC preparations with varying levels of oxygen saturation. There was no relationship between oxygenation status of infused Ngb-H64Q-CCC and the extent and rate of CO-Hb clearance (Table S1), consistent with our in vitro findings and computational models (Fig. 2, 3).

To compare the efficacy of Ngb-H64Q-CCC with 100% normobaric oxygen, widely used as a standard treatment for CO poisoning, mice were exposed to 100% normobaric oxygen after CO exposure. CO-Hb levels dropped after the first 5 min by an average of 35.0 ± 2.1% in the group that received Ngb-H64Q-CCC and by 27.4 ± 1.6% in the group that received 100% oxygen inhalation (n = 5) ($P < 0.05$) (Fig. 4E), suggesting Ngb-H64Q-CCC is more potent in CO removal from mouse RBCs than is normobaric oxygen. Note that CO elimination in mice under normoxia and 100% oxygen is over 20 times faster than CO elimination in humans, while the removal rates with exposure to Ngb-H64Q-CCC differ only by 3-fold between mouse and human RBCs (Fig. 3I). This suggests that Ngb-H64Q-CCC will be a much more effective treatment for CO poisoning than is oxygen therapy in humans.

Ngb-H64Q-CCC restores blood pressure, improves tissue oxygen delivery and increases survival in a lethal CO poisoned mouse model

We developed a lethal, CO poisoning mouse model to test whether Ngb-H64Q-CCC increases survival after CO exposure compared with controlled infusions of PBS. To stabilize respiration during CO exposure and allow for the direct evaluation of cardiovascular collapse, the most common clinical presentation of severely poisoned patients (4, 7), the exposures were performed in mice on continuous mandatory ventilation with 21% oxygen. After stabilization, mice were exposed to 3% CO and 21% oxygen, balanced with nitrogen, for 4.5 minutes, followed by ventilation with room air (21% oxygen, 79% nitrogen), and the Ngb-H64Q-CCC preparation or same volume of PBS or albumin controls were infused for 2 minutes (Fig. 5A). In these experiments, the concentration of Ngb-H64Q-CCC was 11.6 ± 0.6 mM with the met-Ngb form maintained at only 4.09 ± 1.55% by adding sub-stoichiometric sodium dithionite. Ngb-H64Q-CCC was delivered as 125.4 ± 7.2 nmol/g mouse weight in an infusion volume of 10 μl/g mouse weight. After infusions, the heart rate (HR) in the control mice started to drop 3 minutes after the start of CO poisoning from 269.2 ± 44.6 to 143.9 ± 49.2 beats per minute (BPM). The HR continued to drop in control treated mice, while it started to increase in less than 1 minute after Ngb-H64Q-CCC infusion (Fig. 5B, C). The MAP dropped and continued to decrease to unmeasurable values in the control groups, while MAP increased to the pre-poisoning baseline after Ngb-H64Q-CCC treatment (Fig. 5B, C). Only 10% of the mice survived in the PBS group (n =10) and none survived in the albumin group (n = 7), with median survival times of 24.5 and 23 minutes, respectively. In the Ngb-H64Q-CCC treated group, 87.5% mice (n = 8) survived to the pre-specified protocol sacrifice time of 40 minutes (Fig. 5D; $P = 0.0008$).

CO-Hb levels in the blood were measured before and after the infusions in separate experiments with different mice. There was a greater drop in CO-Hb after infusion in the Ngb-H64Q-CCC treated group than in either control group (33 ± 0.49 % in Ngb-H64Q-CCC vs. 4.66 ± 1.05 % in PBS vs. 11.08 ± 0.96 % in albumin, $P < 0.0001$, Fig. 5E), suggesting that Ngb-H64Q-CCC increased the rate of CO removal from Hb and restored the oxygen binding capacity of Hb, which may have contributed to the improved survival. We also measured CO-Ngb in plasma at the same time points.

Blood Ngb was almost fully saturated with CO immediate after the infusion (99.87 ± 0.20% CO-Ngb measured in plasma), with a Ngb-H64Q-CCC concentration of 1.17 ± 0.06 mM in the mouse plasma. The concentration of Ngb-H64Q-CCC in plasma decayed from 1170 ± 60 μM at the end of the infusion to 271 ± 32 μM at the end of experiment (Fig. S7). A fit of the decay of the Ngb-H64Q-CCC concentration in plasma to a single exponential equation yielded an observed rate of 0.053 ± 0.022 min^{-1}, corresponding to an estimated plasma half-life of 13.1 min (Fig. S7), consistent with the rapid renal excretion of the CO-bound molecule.

To understand the effects of Ngb-H64Q-CCC on tissue oxygen delivery (31) in CO poisoning, lactate measurements were performed serially after infusion of treatment and control animals (Ngb-H64Q-CCC, PBS or albumin). The infusion of Ngb-H64Q-CCC significantly lowered lactate levels in mice at both 24.5 and 40 minutes after exposure: (24.5 min: 5.77 ± 0.86 mM; 40 min: 9.17 ± 0.44 mM) vs. PBS (24.5 min: 10.67 ± 1.53 mM; 40 min: 14.07 ± 0.33 mM; time $P < 0.0001$; treatment $P = 0.0461$; interaction $P = 0.0022$) and albumin (24.5 min: 9.6 ± 0.20 mM; 40 min: 13.0 ± 0.32 mM; time $P < 0.0001$; treatment $P = 0.0376$; interaction $P < 0.0001$) (Fig. 5F). These findings have potential clinical relevance because low pH from lactic acidosis is prognostic of poor outcome in patients with severe CO poisoning (1).

Toxicological assessment of Ngb-H64Q-CCC in a mouse 48-hour survival model

In our study, CO-Ngb-H64Q-CCC was rapidly cleared from blood to urine, indicating that the kidney filters the protein, similar to the process of Mb clearance after rhabdomyolysis (32). To evaluate the potential toxic effects of this Ngb mutant protein *in vivo*, we performed an *in vivo* toxicological study in mice exposed to 4,000 ppm CO for 15 minutes, an exposure level that increases mouse blood CO-Hb levels to approximately 67 ± 5.2% of total Hb and is not lethal. For these survival studies, the drug was delivered by retro-orbital injection of 250 μl of 9–10 mM Ngb-H64Q-CCC, and mice were sacrificed 48 h later for collection and analysis of blood, kidney, liver, heart, brain and lung. The retro-orbital route of delivery was used to limit surgical vascular manipulation for this study. All mice that received Ngb-H64Q-CCC (n = 4) or PBS only (n=4) were alive 48 h after the experiment. Complete blood counts (CBC) and blood chemistry (including creatinine, AST/ALT) for Ngb-H64Q-CCC-treated mice revealed normal values, suggesting that Ngb-H64Q-CCC does not impair renal or liver function in mice (Fig. S8). Furthermore, kidney histology was normal, and Western blot analysis did not detect Ngb in liver, kidney, heart, brain and lung tissues. As a positive control, we also tested 10 mM met-Ngb-H64Q-CCC and found that this oxidized molecule that cannot bind CO is entrapped in the organs and produces organ injury (Fig. S8).

DISCUSSION

In the present studies, we characterized the biophysical properties of a mutant five-coordinate neuroglobin, Ngb-H64Q-CCC. This molecule exhibited a very high CO association rate (k_{on}) and equilibrium association constant (K_A) relative to Hb; it also had a high M-value (K_A CO/K_A O_2), but relatively low autoxidation rates. These properties promoted rapid CO scavenging from Hb and RBCs in vitro, and in CO-poisoned mice

increased CO elimination rates and improved hemodynamics, lactic acid levels and survival. Thus, a high-affinity globin variant can successfully scavenge CO in vivo in mice. That such a variant may prove useful to treat CO poisoning in humans is supported by reports of a naturally occurring hemoglobinopathy, hemoglobin Zürich, in which the CO affinity of the mutant Hb Zürich is approximately 65 times greater than that of normal Hb. Like our mutant Ngb, this variant also carries a mutation of the distal histidine of the Hb beta chain (H63R) (33).

Rapid confirmation of CO poisoning and continuous monitoring of CO-Hb, which can now be performed non-invasively in the field with pulse CO oximetry, allows for triage and transfer of poisoned patients to facilities with hyperbaric oxygen “dive chambers”. Exposure of patients to 100% normobaric or hyperbaric oxygen, the only current therapeutic options, reduces the elimination half-life of human CO-Hb from 320 minutes to 74 and 20 minutes, respectively (1, 7, 34–36). However, in practice the efficacy of hyperbaric oxygen therapy is often limited because of time delays between diagnosis, transportation to a hyperbaric center, and treatment (1, 6, 7, 37–40). Moreover, the most unstable patients usually require mechanical ventilation and intensive care support, which are not easily administered within a hyperbaric capsule. Even with effective hyperbaric therapy, a significant portion of patients who survive CO poisoning suffer from long term neurologic deficits. Neurocognitive sequelae persist in 13–37% of patients for up to 6 years after initial poisoning (38, 41).

Recombinant Ngb-H64Q-CCC may be rapidly administered as an antidote to CO poisoning in the field or in the emergency room, with calculated and measured clearance half-lives of less than a minute from RBC Hb. Placement of an intravenous angiocatheter and delivery of recombinant Ngb-H64Q-CCC would be anticipated to immediately decrease the CO-Hb levels by ≈ 7–10% for every 1 g/dL administered. Although our studies evaluated efficacy and safety only in mice, similar amounts of Hb-based blood substitutes have been used in Phase 1 clinical trials in trauma and surgical patients (50–100 g), suggesting potential feasibility for this dosing in humans (42–44).

Other approaches for treating CO poisoning are in the early stages of development (7). These include phototherapy with light exposure to increase the rate of CO release from hemoglobin (45), hydroxocobalamine to metabolize CO to carbon dioxide (46), and a synthesized water-soluble supramolecular complex (hemoCD) which, when infused in rats, scavenged CO from the rat body and the CO-bound hemoCD was immediately excreted in the urine (47).

What causes the lethal effects of CO? The formation of CO-Hb and an associated decrease in oxygen transport originally was considered to be the major mechanism of CO toxicity (2, 3). However, the clinical severity in CO-poisoned patients does not directly correlate with blood CO-Hb levels (5, 37), and clinical improvement does not correlate with the rate of clearance of blood CO-Hb. Also, as observed in canine studies, the toxicity of a particular concentration of CO is greater when CO is administered by inhalation rather than by transfusion of CO-exposed RBCs (48). These studies suggest that CO-Hb levels serve as a crude measure of CO exposure, but the lethal effects result from the global impact of both reduction in Hb oxygen delivery and the direct inhibition of mitochondrial respiration in

tissues. It is now well appreciated that CO poisoning causes tissue ischemia-reperfusion injury, mitochondrial dysfunction and damage, cellular necrosis and apoptosis and down-stream activation of immunological and inflammatory events. CO inhibits mitochondrial respiration by binding the ferrous heme of cytochrome *c* oxidase (Complex IV), effectively shutting down oxidative phosphorylation, similar to the effects of cyanide (48–50). Thus removal of CO from the circulation is important as it will limit the continuous delivery of CO to the tissues, but removal of CO from the mitochondria is also required to further diminish CO toxicity. Our observations of rapid improvements in heart rate, blood pressure and lactate levels upon administration of Ngb-H64Q-CCC indicate a therapeutic effect of CO scavenging, consistent with reductions in blood CO levels and improved oxygen delivery and utilization in affected organs.

Major complications of acellular Hb-based blood substitutes used as oxygen delivery molecules, which have been tested in humans, were hypertension and multi-organ injury caused by both NO scavenging and heme-mediated oxidative reactions (51–54). There are, however, factors that may limit these complications for Ngb-H64Q-CCC treatment of CO poisoning. First, the concentration of CO-Hb in these patients will be higher than the concentration of infused Ngb-H64Q-CCC and several orders of magnitude higher than the endogenous NO concentration. CO levels of >30% CO-Hb in our studies are greater than 2 mM, while NO concentrations *in vivo* are orders of magnitude lower (55). Thus CO is expected to outcompete NO for binding to the infused Ngb-H64Q-CCC, limiting NO-mediated responses. Second, in the presence of CO, Ngb-H64Q-CCC binds CO almost irreversibly. Upon CO removal, Ngb-H64Q-CCC will be mostly CO-bound, thus blocking possible NO dioxygenation reactions, Fenton reactions, and lipid-peroxidase reactions that scavenge NO and generate reactive oxygen species. As revealed by our 48 h survival and safety study (Fig. S7), all mice with moderately severe CO poisoning that received deoxy-Ngb-H64Q-CCC injection remained alive with normal renal and liver function, while the mice given met-Ngb-H64Q-CCC (which lacks CO binding capacity) exhibited trapped met-Ngb-H64Q-CCC in the kidney, and showed abnormal liver and kidney function (Fig. S8). Third, Ngb-H64Q-CCC has a nitrite reductase rate constant ≈2,500 times faster than that of Hb (Fig. S4), suggesting that the molecule may generate NO from plasma nitrite and potentially offset effects of NO scavenging (12, 18). Blood pressure in mice receiving Ngb-H64Q-CCC was restored to nearly pre-exposure levels as compared with mice that were infused with PBS, while no hypertension was observed. Moreover, hemodynamic improvements in response to Ngb-H64-CCC infusion compared to PBS were observed in the lethal poisoning model (Fig. 5B, C), without seeing increases in blood pressures above baseline values, indicating no true hypertensive effects.

There are a number of limitations inherent to our studies in mice. We measured CO clearance, hemodynamics and mortality, but have not tested long term effects on neurocognitive dysfunction, one of the major complications in humans with CO poisoning. We have also assessed cellular metabolism using a surrogate marker, lactic acid, rather than direct measurement of mitochondrial respiration. Further safety and efficacy studies in large animal models are needed to advance this therapy toward treatment of CO poisoning in humans.

In conclusion, the current studies support the development of recombinant Ngb as a biological therapeutic. Despite recognition of the role of Ngb in cellular cytoprotection, this molecule has not previously been harnessed as a therapeutic. In addition to CO scavenging and oxygen delivery, Ngb may have other useful effects on cellular function via cytochrome c reduction or nitrite reduction to form NO (11–13, 18). The triple cysteine substitutions to the H64Q Ngb reduce intramolecular cross-linking and increase protein solubility, allowing for the preparation of stable >12 mM stock solutions. High concentrations of Ngb could allow for "unit" infusions of saline containing 50 – 100 g of Ngb in the field by paramedics, necessary to increase the plasma levels to 1 – 2 g/dL and stoichiometrically scavenge CO from CO-Hb complexes (56), which would reduce the CO-Hb level by an absolute percentage of approximately 10–15% (e.g. from 30% CO-Hb to 15–20%). Our studies identify a potential antidotal therapy for CO poisoning that, if proven safe in large mammals and humans, could be given in the field by paramedics to rapidly scavenge CO from RBCs, tissues, and heart within minutes, providing a potential life-saving approach to the most common human poisoning.

MATERIALS AND METHODS

Study design

The objective of this study was to investigate the ability of a mutant five-coordinate Ngb mutant with very high CO binding affinity to serve as a CO scavenger for the treatment of CO poisoning. We characterized the CO and oxygen binding affinity of the mutant Ngb and monitored the rates of CO transfer from free Hb and RBCs to the mutant Ngb *in vitro*. We developed non-lethal and lethal CO poisoning mouse models to monitor the effect of Ngb mutant infusions on CO clearance, hemodynamics and survival rate. All the *in vitro* experiments were repeated at least three times. All animal studies were performed using protocols approved by the Institutional Animal Care and Use Committee at the University of Pittsburgh and in accordance with National Institutes of Health guidelines. Randomization of animals into the study was based on body weight to ensure equal distribution across groups. No statistical method was used to predetermine sample size for all experiments. Investigators were not blinded to experiments. All data are included (no outlier values were excluded).

Reagents and standard sample preparation

Blood was used freshly or up to 4 weeks after collecting from human volunteers and Hb was prepared as described previously(53). Mouse blood was collected from C57BL/6 mice and used within 10 days. All chemicals were purchased from Sigma unless otherwise noted. All concentrations of pre-mixed CO gas were purchased from Matheson Inc. and were confirmed by Testo combustion analyzer 320 in our lab. Visible absorbance spectra and kinetic data were collected on a Cary 50 and a HP8453 UV-visible spectrophotometer (Agilent Technologies). All experiments were performed in PBS, (Sigma). CO-saturated buffer was prepared by bubbling 10–20 mL of PBS with CO gas for at least 30 minutes. Stock sodium dithionite solution was prepared by adding PBS degassed by Argon flow-through to a degassed vial of dry sodium dithionite.

Neuroglobin expression and purification

Site-directed mutagenesis of the wild type Ngb to H64Q and H64Q combined with three surface thiol substitutions (a C46G, C55S, and C120S mutation), referred to as Ngb-H64Q and Ngb-H64Q-CCC, respectively, was performed using QuikChange II kit (Stratagene), as described previously (12, 14) For expression, cDNA was cloned in the *E. coli* competent cells Rosetta 2(DE3) or BL21 (DE3) from Novagen, with the Ngb-H64Q-CCC gene carried by pET-28 plasmid (Novagen). A 25% glycerol stock of the cells was stored at −80 °C. Expression of cells grown in LB broth at 37 °C was induced upon reaching OD_{600} of 0.9 with 1mM isopropyl 1-thio-β-D-galactopyranoside and included δ-aminolevulinic acid (0.4 mM) in the media. Expression of cells grown in autoinducing media (57) was induced upon reaching OD_{600} of 0.45 by switching incubation temperature from 37 to 18 °C. 30 μg/ml Kanamycin was added to media containing either BL21 or Rosetta cells while 34 μg/ml Chloramphenicol was added only to the Rosetta cells. For cells in autoinducing media, the incubation temperature was raised from 18 to 30 °C the next day (after ~20 h) and they were grown for an additional ~ 7 h. Cells were harvested on the third day at 11000 × g for 10 min in 500 mL centrifuge bottles, weighted and either frozen at −80 °C or lysed immediately for purification.

Cells were lysed in 50 mM MOPS (pH 7.0) containing 1 mM EDTA, 1mg/ml lysozyme, 1 mM PMSF and 0.5 mM DTT, filtered using 0.22 μm SteriTop vacuum filters (Millipore) and loaded unto an HPLC DEAE anion exchange column. The bound protein was then washed with 10 mM NaCl followed by 30–35 mM NaCl (in 50 mM MOPS), each time washing until absorbance intensities at 215 and 280 nm decreased back to baseline. The protein was then eluted with a gradient to 115 mM NaCl in approximately one column volume, monitored via absorbance at 415 nm. Fractions were pulled together and concentrated using 30 KDa Centricon centrifugal filter units (Millipore) to 3 mL or less. The concentrated protein was passed through a 0.22 μm filter, loaded onto an HPLC gel filtration column and eluted (Absorbance of protein monitored at 415 nm). The eluted fractions were again pulled together and endotoxins were removed with Pierce High Capacity Endotoxin Columns. To further decrease the endotoxin levels, an extra step of hydrophobic capture using a Butyl-HP sepharose column (GE Healthcare) was eventually included. Protein samples were loaded in 50 mM sodium phosphate buffer (pH 7.2) with 2 M NaCl. The protein was washed with the same buffer and then eluted with a gradient from 50 mM sodium phosphate buffer (pH 7.2) with 2 M NaCl to 10 mM sodium phosphate buffer (pH 7.2) without NaCl.

After endotoxin removal, an excess amount of ferricyanide was added to oxidize the protein and removed by a gravity size-exclusion column (Econopac 10DG, BioRad). For *in vitro* experiments, the oxidized protein was concentrated and frozen at −80 °C. SDS-PAGE was used as purity criteria. The protein yields were similar to wild type Ngb and we do not observe significant stability changes (i.e. protein aggregation) in the 4–37°C temperature range. For *in vivo* experiments, the protein was further reduced by an excess amount of sodium dithionite. For infusions of deoxy-Ngb-H64Q-CCC, the sodium dithionite was removed by a gravity size-exclusion column (Econopac 10DG, BioRad) inside an anaerobic globe box. The protein was then concentrated inside the glove box, sealed inside anaerobic glass vials and frozen at −80 °C. For infusing oxy-Ngb, the sodium dithionite was removed

from the protein at 4 °C in atmospheric conditions. The Ngb was then concentrated, in atmospheric conditions, at 4 °C to slow down autoxidation and frozen at −80 °C. Then, the protein, was exposed to cycles of vacuum and nitrogen gas to remove dissolved oxygen, sealed in glass vials, and replaced at −80 °C.

Preparation of reduced, oxidized and ligand bound neuroglobin and hemoglobin

Thawed Ngb-H64Q-CCC was mixed with an excess of potassium ferricyanide and passed through a desalting column to obtain the oxidized (met) form. Ferrous deoxy-Ngb was obtained by adding an excess of sodium dithionite to the oxidized form. For aerobic experiments, the oxygen-bound form was obtained by passing the ferrous deoxy form through a desalting column (PD spin trap G-25, GE Healthcare) under aerobic conditions immediately before mixing with CO-Hb. CO-Hb was obtained by adding an excess of sodium dithionite to degassed, oxygen-bound Hb and diluting with PBS containing an excess of dissolved CO. To remove remaining dissolved CO the CO-Hb solution was passed through a desalting column inside an anaerobic glove box and sodium dithionite was added back to CO-Hb in case of anaerobic experiments.

Preparation of apo-neuroglobin

Heme-free Ngb was prepared by the acid-acetone method as previously described (58). A solution of acetone (100ml) was acidified with 1ml of 2M HCl and pre cooled to −20 °C. 50 μl of Ngb-H64Q-CCC 10mM were added to the acetone solution under stirring. The solution was centrifuged at 10000× g for 5 min and the precipitate was resuspended again in acidified acetone until clear. The white precipitate was finally resuspended in cold water and buffer exchanged using 10 KDa Centricon centrifugal filter units (Millipore) first to 0.1% sodium bicarbonate in water and then to PBS. The final concentrated protein was centrifuged at 16000× g for 5 min to remove any insoluble protein. The concentration of the protein was assessed in 6M guanidine hydrochloride using an extinction coefficient of 22190 $M^{-1}cm^{-1}$ at 280 nm according to Edelhoch (59).

Determination of neuroglobin CO and Oxygen binding affinities

Flash photolysis was used to determine the on-rate of CO on Hb and both Ngb mutants. Standard spectra determined as described in the “Least squares deconvolution” section were used to monitor the species formed during the reaction. For these experiments, the samples of wild type and recombinant Ngbs (described below) and Hb are saturated with CO gas and then were photolysed with a 20 mJ 6ns Nd-YAG laser pulse at 532 nm and the CO recombination kinetics were recorded using an extremely fast streak camera which collects spectral data with submicrosecond time resolution, with fits to first order kinetics using global analysis employing SpecFit software (27, 28, 30). Each protein was diluted into a phosphate buffer containing 10 mM sodium dithionite that had been de-gassed with CO. The samples remained under CO pressure for an additional 15 minutes and then were photolysed. The recombination kinetics was recorded for 1200μs and 100μs for Hb and Ngb, respectively. The resultant absorption difference spectra (transient minus ground state) was fit to first order kinetics using global analysis employing SpecFit software (60). To further investigate the binding kinetics, the Ngb-H64Q-CCC was incubated under 0.1 atm CO and the above assay was repeated with the same laser parameters. The time scale was changed to

0–3 ms and 0–6 ms for Ngb and Hb, respectively. The bimolecular rate constant for oxygen binding was determined similarly as that for CO binding and as described previously (61). Ngb-H64Q-CCC was equilibrated with one atmosphere of CO (200 μM Ngb and 1 mM CO). This sample was diluted 1:10 in air-equilibrated phosphate buffered saline so the final concentration of Ngb-H64Q-CCC was 20 μM and the final oxygen concentration was 225 μM. The laser was used to photolyse CO and oxygen recombination kinetics were observed for 30 μs following photolysis.

Absorption spectroscopy kinetics was used to determine the off-rate of CO on both Ngb mutants, as well as Hb. Samples of 10μM protein and 100μM sodium dithionite were saturated with CO. Then 1mM NO solution was prepared using ProliNONOate (Cayman Chemical # 82145) and was injected into each sample and immediately scanned on a Cary50 spectrophotometer. Absorption spectra were recorded for 45 minutes and 270 minutes for Hb and Ngb, respectively. The data was once again fit to first order using SpecFit software.

Determination of oxygen dissociation kinetics

The rate of oxygen dissociation from Ngb-H64Q-CCC was determined by ligand replacement. The experiments were carried out at 25 °C in an Applied Photophysics SX-20 stopped-flow spectrophotometer with a diode array detector (Applied Photophysics Ltd.) contained in an anaerobic glove box (Coy Laboratory Products). 100 mM sodium phosphate buffer, pH 7.4 was used for all the solutions. The Ngb samples were reduced by excess sodium dithionite in the glove box and the deoxy-Ngb was run through a gravity size-exclusion column (Econopac 10DG, BioRad) to remove the excess of reductant. The protein was mixed with air-saturated buffer ($[O_2] \approx 260\mu M$) in 1:4 (v/v) or 1.5:1 (v/v) ratios to form quantitatively the Ngb-oxy complex and achieve final oxygen concentrations of ≈ 208 μM (1:4) or ≈ 104 μM (1.5/1). This sample was then mixed different concentrations of CO buffer made by mixing CO-saturated buffer ([CO] ≈ 1 mM) and anaerobic buffer in the stopped-flow instrument. The spectrum in the visible range (350–730 nm) was sampled every 1.24 ms for a reaction time of 1 s. Spectral changes were consistent with a decay of the Ngb-oxy complex to form the Ngb-CO species. Traces over the whole spectral range (300–730nm) where fitted simultaneously for each experiment using the Pro-K software (Applied Photophysics Ltd.) to calculate the observed oxygen dissociation rate.

Hemoglobin-to-neuroglobin CO transfer kinetics

Free Hb kinetics—CO-Hb was prepared by adding an excess of sodium dithionite to thawed Hb and mixing with CO-saturated buffer in a ratio of at least 1:4 (1 volume of Hb to 4 volumes of CO saturated buffer). Excess CO was removed by passing through a desalting column inside an anaerobic glove box. For anaerobic experiments an excess of sodium dithionite was then added to the CO-Hb. To measure CO transfer kinetics, CO-Hb inside a cuvette of 1 cm path length was placed in the cell holder of a Cary 50 spectrophotometer at 37 °C. The reaction was initiated by injecting Ngb into the CO-Hb solution for a final concentration of 30 – 40 μM of both proteins.

Red Blood Cell kinetics—RBCs were obtained by washing 50 – 100 μL of packed RBCs with PBS 3 to 5 times by centrifugation at 2000 × g for < 1 min. The washed RBCs were

diluted in 1 to 2 ml of PBS and deoxygenated while on ice and slowly stirring by a passing flow of argon gas for up to 60 min. Sodium dithionite was then added to the RBCs such that the concentration after dilution in CO-buffer would not exceed 7 mM. RBC-encapsulated CO-Hb was obtained by diluting the deoxygenated RBC solution with a ratio of at least 4:1 (v/v) of CO buffer to RBCs. Excess CO was removed by diluting the RBCs 5-fold with de-gassed PBS (containing 5 – 10 mM sodium dithionite for anaerobic experiments), followed by centrifugation and removal of the supernatant. Afterwards, the RBCs were resuspended to a final concentration of 100 – 300 μM in heme, with an excess of sodium dithionite for anaerobic experiments. RBCs with 100% CO-Hb were equilibrated to 37 °C in a 1 cm septum-capped cuvette inside the cell holder of a Cary 50 spectrophotometer and the reaction was initiated by injecting Ngb-H64Q-CCC into the RBC solution. Sets of experiments with ratios of Ngb to Hb of 0.5, 1, 1.5 and 5.6:1 (in heme) were performed. The reaction mixture contained 2–10 mM sodium dithionite under anaerobic conditions, while under aerobic conditions the cap was removed from the cuvette before injecting Ngb-H64Q-CCC. All reaction mixtures were stirred continuously. 0.3 mL samples were removed from the reaction mixture in immediate succession and, after centrifugation, supernatants were removed and saved in pre-labeled microcentrifuge tubes, while 0.3 mL of 10 mM sodium dithionite with 0.5% NP40 in PBS was added to the RBC pellets for cell lysis and absorbance measurement. Absorbance measurement of the saved supernatants and lysed RBC pellets was initiated immediately after centrifugation of the last time point. Control experiments were performed similarly, but without addition of Ngb mutants.

Mouse hemoglobin preparation

Mouse Hb were prepared as reported for human Hb (26). In short, mouse RBCs were washed with PBS, and lysed hypotonically by dilution with excess H_2O. The lysed RBCs were centrifuged at 7000 × *g* to remove cell debris. The resulting solution, consistent of mostly Hb, was concentrated and buffer exchanged using Amicon Ultra centrifugal filters (Millipore) with a cutoff of 50 kDa in order to remove low molecular weight contaminants. Samples were aliquoted and frozen in liquid N_2 and stored at −80°C.

Least squares deconvolution

Standard reference spectra of the oxidized (met), ferrous (deoxy), oxygenated (O_2-bound), carboxy (CO-bound), and nitrosylated (NO-bound) forms of human Hb, mouse Hb and Ngb were obtained. The reference species for each species were obtained as follows: after thawing protein on ice, spectra of the oxidized species were obtained by mixing with an excess of potassium ferricyanide and passing through a gravity size-exclusion column (Econopac 10DG, BioRad). Spectra of deoxy species were recorded after adding an excess of sodium dithionite to the oxidized form (2 – 5 mM). Spectra of the oxygenated form were recorded immediately after passing a sample of the deoxy species through the size-exclusion column under aerobic conditions at 4 °C.

Spectra of the CO-bound species were measured after mixing the deoxy proteins with CO-saturated buffer in a ratio of 1:4. Spectra of the nitrosylated (NO-bound) species were obtained as for the CO-species adding NO-saturated buffer instead of CO-saturated buffer. All standard spectra were collected on a Cary 50 spectrophotometer. Spectral deconvolution

of time-resolved absorption data collected at 22, 25 or 37° C was performed by a least squares fit using basis spectra as described previously (12, 27–30). We used two methods to evaluate the accuracy of the deconvolution. First, we kept the total concentration of Hb/Ngb constant through the reaction based on the initial concentration. Secondly, the results were double checked by fitting the spectra in two different wavelength ranges, typically 490 to 650 and 450 to 700. For both Hb and Ngb-H64Q-CCC the oxidized and diatomic ligand-bound forms were also converted to denatured forms, which have the same absorbance spectra of an oxidized heme, with the QuantiChrom Heme Assay Kit (BioAssay Systems). All of the basis spectra were standardized to an absorbance of $mM^{-1}cm^{-1}$ using an extinction coefficient of 68.1 $mM^{-1}cm^{-1}$ of the oxidized heme. This extinction coefficient was calculated by converting the same solution of met-globin to the denatured, oxidized heme, form and to cyanomet heme. The extinction coefficient used for cyanomet heme was 11 $mM^{-1}cm^{-1}$ at 540 nm (62) Deconvolution of experimental spectra was performed with a least-squares fitting routine in Microsoft Excel. Because the change in absorbance of some kinetic experiments is small, all spectra composed of both Hb and Ngb-H64Q-CCC were always fit between 450 and 700 nm, 490 and 650 nm, and 510 and 600 nm; with and without constraining the Hb and Ngb-H64Q-CCC concentrations to be equal to each other (for equimolar experiments) and to their pre-calculated concentrations, in order to confirm the accuracy of the deconvolution. For the same purpose, sometimes, a parameter that could shift the spectra horizontally, along the wavelength axis, was also included in the fit (not used in any of the data shown). Absorbance spectra from anaerobic experiments were deconvoluted using CO- and deoxy- standards of Hb and Ngb-H64Q-CCC.

Absorbance spectra from aerobic experiments were deconvoluted using the standards of the oxidized, CO-bound and oxygenated forms of Hb and Ngb-H64Q-CCC. For the RBC experiments where Hb was separated from Ngb and sodium dithionite was afterwards added to either RBCs in aerobic experiments or to the supernatant in anaerobic experiments, deoxy standards were used in deconvolution instead of the oxy- and met- forms.

Modeling of neuroglobin structures

The structure of wild type human Ngb was modeled using the Swiss model server (63) with the reported structure for the C46G/C55S/C120S mutant (PDB:1OJ6) (64) as template. The unliganded Ngb-H64Q structure was modeled using the PyMOL mutagenesis tool (65) on the previous model for the Ngb wild type structure. The Ngb-H64Q model with bound CO was built from the CO-bound wild type Ngb structure (PDB: 1W92) (66) using the PyMOL mutagenesis tool (65) to introduce the H64Q mutation.

Non-lethal CO poisoning mouse model

Male C57BL/6 wild-type mice (10–12 week) were obtained from The Jackson Laboratory (Bar Harbor, ME). All studies were performed using protocols approved by the Institutional Animal Care and Use Committee at the University of Pittsburgh and in accordance with National Institutes of Health guidelines. Mice were anesthetized with inhaled 2% isoflurane, and micro-renathane catheters (MRE-025; Braintree Scientific) were inserted into the left femoral artery and vein, sutured in place, stabilized with superglue, tunneled subcutaneously to exit the skin at the upper back, taped to a wire attached to posterior cervical muscles for

stiffness (792500; A-M Systems), and connected to a 360 degree dual channel swivel designed for mice (375/D/22QM; Instech).

Catheter patency was maintained by continuous sterile infusion of 7ul/h saline containing 20 units/ml heparin (APP Pharmaceuticals) using a syringe pump with multisyringe adaptor (R99-EM; Razel Scientific Instruments). CO exposure was performed in conscious mice after three days recovery from catheter implantation. Mice were randomly allocated to PBS or Ngb treatment with similar body weight without blinding. Mice were exposed to 1500 ppm of CO equilibrated in 21% oxygen and 79% nitrogen (Matheson Inc.) in an individual customized chamber in which gas entered through inlet ports in the base and exhausted through an open hole at the apex (67). Blood samples for CO-Hb measures were collected by first drawing a 70 μL volume from the arterial catheter to clear the dead space, followed by 20 μL of blood (by a different 25 μL syringe) at various time points. 5 μL of the drawn blood were washed and the absorbance spectrum was immediately measured at 200-fold dilution and deconvoluted to calculate the percentage of CO-Hb out of the total amount of Hb (CO-Hb%). After an average 50 minutes of CO exposure, the animals were returned to normal atmospheric conditions and a 275 μL infusion (delivering 250 μL to the animals) of either PBS or Ngb-H64Q-CCC was started for 4 minutes through venous catheter. Blood samples were collected every 10 minutes during CO exposure, every 5 minutes for 30 min after exposure and again every 10 minutes until the CO-Hb levels decreased below 10%. At this point the animals were sacrificed and urine (if present) was immediately drawn from the bladder for analysis. Blood sample supernatants were stored on dry ice until after the end of an experiment, when measured via absorption (to check for cell lysis via presence of Hb and for CO-Ngb).

In the toxicological study, male C57BL/6 wild-type mice were exposed to 4000 ppm for 15 minutes. Ngb-H64Q-CCC was administrated at 9–10mM in 250ul by retro-orbital injection after CO exposure and mice were sacrificed at 48 h for blood and tissue collection (kidney, liver, heart, brain and lung). Fresh blood samples were sent for tests of complete blood counts (CBC, Hemavet 950FS) and plasma samples were sent for blood chemistry panel test (including creatinine, AST/ALT, urea and phosphorus).

Lethal CO poisoning mouse model

Male C57BL/6 wild-type mice were used at a mean age of 10–13 weeks and, mean weight of 23.4–27.4 g. The experimental protocol was approved by the Institutional Animal Care and Use Committee at the University of Pittsburgh and in accordance with National Institutes of Health guidelines. Ngb-H64Q-CCC was reduced anaerobically by excess sodium dithionite, removed by a gravity size-exclusion column (Econopac 10DG, BioRad) and concentrated with Amicon Ultra centrifugal filters (0.5 ml, 10 KDa cutoff, Millipore). Sodium dithionite was added at substoichiometric concentrations to the Ngb-H64Q-CCC after desalting so that its concentration was between 1.25 to 2.5 mM. Ngb-H64Q-CCC concentration and the percentage of met-Ngb was confirmed spectrophotometrically, with least-squares deconvolution using component reference spectra. The Ngb-H64Q-CCC solutions of 11.6 ± 0.6 mM with the met-Ngb-H64Q-CCC form maintained at only 4.09 ± 1.55% in an infusion volume of 10 μl/g mouse weight were loaded into a 1ml insulin

syringe (U-100, BD) anaerobically, the needle sealed with rubber, and frozen at −80°C until ready for infusion. Albumin (5 mM) and PBS were used as controls with sodium dithionite concentration of 2.5 mM. The mice were anesthetized by isoflurane, a tracheal tube placed followed by cannulation of right jugular vein and left carotid artery. Arterial blood pressure was monitored and recorded (DATAQ instruments) through a catheter in the carotid artery. An intravenous catheter was placed and used for Ngb-H64Q-CCC or control PBS infusions using a syringe pump. Infusion volume was calculated according to the mouse weight (10 μl/g) and dead volume of the catheter.

Ventilation was initiated after the surgery with a volume controlled ventilator (MiniVent, Type 845; Hugo Sachs). Air was administrated (21% oxygen) with 1.5% isoflurane at tidal volumes of 228 ~ 270 μl (8.8 μl/g weight) and respiratory frequencies of 175 BPM. Three percent (3%) CO was delivered in air for 4.5-minutes via the ventilator. After CO delivery the ventilator delivered air without CO and the Ngb-H64Q-CCC or PBS control was infused for 2-minutes. Arterial blood pressure and heart rate signals were processed using Labchart software (ADInstruments Ltd.). Mortality was established based on an unmeasurable heart rate and blood pressure for 5 minutes and all mice were followed for a pre-defined experimental observation period of 40-minutes from CO exposure, followed by sacrifice.

Blood lactate analysis in the lethal CO poisoning model

Using the lethal CO poisoning mouse model, we measured the lactate levels as a marker of tissue perfusion and oxygen delivery. Blood was withdrawn from the arterial catheter in the carotid artery at the following time points: prior to the commencement of the infusion of treatment with PBS, albumin or Ngb-H64Q-CCC (level drawn between 4.5 and 6.5 minutes). 9.5, 14.5, 19.5, 24.5 and 40.0 minutes from the commencement of CO exposure. Lactate was measured using the Lactate Plus Professional Lactate Reader (Lactate.com), results are reported in millimoles per liter (mM).

Western blotting

Mice tissue samples (kidney, liver, brain, heart and lung) were lysed in ice-cold lysis buffer [20 mmol/L Tris pH 7.5, 150 mmol/L NaCl, 1 mmol/L EDTA, 1 mmol/L EGTA, 1% Triton X-100, 2.5 μmol/L Na-pyrophosphate, 1 mmol/L β-glycerophosphate, 1 mmol/L Na3VO4, 1 mmol/L phenylmethylsulfonyl fluoride, 1 μg/mL Complete Protease Inhibitor Cocktail (Roche Applied Science). Protein lysates (100 μg total protein) were separated on a 4–12% SDS Bis-Tris protein gel under reducing conditions, followed by electrotransfer to a nitrocellulose membrane. After blocking, the membranes were probed with rabbit anti-Ngb polyclonal antibody (sc-30144, Santa Cruz Biotechnology, Inc.). Purified Ngb-H64Q-CCC was used as a positive control.

Histology

Mouse kidney tissues were fixed in formalin for 24 h, embedded in paraffin and cut into 4 μm sections. The slides were stained with hematoxylin and eosin (H&E) and examined under light microscope.

Statistical analysis

Data are presented as means ± SEM and were analyzed by unpaired Student's *t*-test or one-way ANOVA unless indicated otherwise. Statistical analyses were performed using GraphPad Prism software version 6.0. A mixed effect model with unstructured covariance was applied to determine time treatment (Ngb vs. PBS) interaction and the effect of treatment after drug infusion (time > 0) for blood pressure data. Two-way ANOVA with repeated measures was performed to determine the effects of treatment (Ngb, PBS, and albumin), time and interaction of these values on lactate levels. P values < 0.05 were considered significant.

Supplementary Material

Refer to Web version on PubMed Central for supplementary material.

Acknowledgments

We thank Venkata Ragireddy and Bonnie Lemster for help with the protein expression and purification. We thank for David Osei-Hwedieh for assistance with mice injection. We also thank Catherine Corey and Erin Schwoegl (University of Pittsburgh) for help with some experiments and Dr. Richard Williams, Crystal Bolden and Lauren Nelson (Wake Forest University Department of Physics) for help with laser flash photolysis experiments. We also acknowledge an anonymous reviewer for the mathematical description of the CO binding process included in Methods section of the Supplementary Materials.

Funding: This work is supported in part by resources provided by the NHLBI SMARTT (Science Moving TowArd Research Translation and Therapy) Program; the Institute for Transfusion Medicine, and the Hemophilia Center of Western Pennsylvania to M.T.G. Additional support was provided by NIH grants F32 HL132418 to J.J.R., R01 HL111706 to C.P.O'D., R01 GM113816 to S.S., R21 ES027390 to J.T., R01 HL058091 to D.B.K.-S., and R01 HL098032, R01 HL125886, P01 HL103455, T32 HL110849, and T32 HL007563 to M.T.G.

REFERENCES AND NOTES

1. Hampson NB, Piantadosi CA, Thom SR, Weaver LK. Practice recommendations in the diagnosis, management, and prevention of carbon monoxide poisoning. Am J Respir Crit Care Med. 2012; 186:1095–1101. [PubMed: 23087025]
2. Bernard, C. Leçons Sur les Effets des Substances Toxiques et Médicamenteuses. Paris: Bailliere; 1857.
3. Haldane J. The relation of the action of carbon monoxide to oxygen tension. J Physiol (London). 1895:201–217.
4. Blumenthal I. Carbon monoxide poisoning. J R Soc Med. 2001; 94:270–272. [PubMed: 11387414]
5. Weaver LK, Valentine KJ, Hopkins RO. Carbon monoxide poisoning: risk factors for cognitive sequelae and the role of hyperbaric oxygen. Am J Respir Crit Care Med. 2007; 176:491–497. [PubMed: 17496229]
6. Weaver LK, Hopkins RO, Chan KJ, Churchill S, Elliott CG, Clemmer TP, Orme JF Jr, Thomas FO, Morris AH. Hyperbaric oxygen for acute carbon monoxide poisoning. N Engl J Med. 2002; 347:1057–1067. [PubMed: 12362006]
7. Rose JJ, Wang L, Xu Q, McTiernan CF, Shiva S, Tejero J, Gladwin MT. Carbon Monoxide Poisoning: Pathogenesis, Management and Future Directions of Therapy. Am J Respir Crit Care Med. in press.
8. Burmester T, Weich B, Reinhardt S, Hankeln T. A vertebrate globin expressed in the brain. Nature. 2000; 407:520–523. [PubMed: 11029004]
9. Bentmann A, Schmidt M, Reuss S, Wolfrum U, Hankeln T, Burmester T. Divergent distribution in vascular and avascular mammalian retinae links neuroglobin to cellular respiration. J Biol Chem. 2005; 280:20660–20665. [PubMed: 15793311]

10. Nienhaus K, Nienhaus GU. Searching for neuroglobin's role in the brain. IUBMB Life. 2007; 59:490–497. [PubMed: 17701543]
11. Raychaudhuri S, Skommer J, Henty K, Birch N, Brittain T. Neuroglobin protects nerve cells from apoptosis by inhibiting the intrinsic pathway of cell death. Apoptosis. 2010; 15:401–411. [PubMed: 20091232]
12. Tiso M, Tejero J, Basu S, Azarov I, Wang X, Simplaceanu V, Frizzell S, Jayaraman T, Geary L, Shapiro C, Ho C, Shiva S, Kim-Shapiro DB, Gladwin MT. Human neuroglobin functions as redox-regulated nitrite reductase. J Biol Chem. 2011; 286:18277–18289. [PubMed: 21296891]
13. Burmester T, Hankeln T. What is the function of neuroglobin? J Exp Biol. 2009; 212:1423–1428. [PubMed: 19411534]
14. Dewilde S, Kiger L, Burmester T, Hankeln T, Baudin-Creuza V, Aerts T, Marden MC, Caubergs R, Moens L. Biochemical characterization and ligand binding properties of neuroglobin, a novel member of the globin family. J Biol Chem. 2001; 276:38949–38955. [PubMed: 11473128]
15. Trent JT 3rd, Hargrove MS. A ubiquitously expressed human hexacoordinate hemoglobin. J Biol Chem. 2002; 277:19538–19545. [PubMed: 11893755]
16. Trevaskis B, Watts RA, Andersson CR, Llewellyn DJ, Hargrove MS, Olson JS, Dennis ES, Peacock WJ. Two hemoglobin genes in Arabidopsis thaliana: the evolutionary origins of leghemoglobins. Proc Natl Acad Sci U S A. 1997; 94:12230–12234. [PubMed: 9342391]
17. de Sanctis D, Dewilde S, Vonrhein C, Pesce A, Moens L, Ascenzi P, Hankeln T, Burmester T, Ponassi M, Nardini M, Bolognesi M. Bishistidyl heme hexacoordination, a key structural property in Drosophila melanogaster hemoglobin. J Biol Chem. 2005; 280:27222–27229. [PubMed: 15917230]
18. Tejero J, Sparacino-Watkins CE, Ragireddy V, Frizzell S, Gladwin MT. Exploring the mechanisms of the reductase activity of neuroglobin by site-directed mutagenesis of the heme distal pocket. Biochemistry. 2015; 54:722–733. [PubMed: 25554946]
19. Nienhaus K, Kriegl JM, Nienhaus GU. Structural dynamics in the active site of murine neuroglobin and its effects on ligand binding. J Biol Chem. 2004; 279:22944–22952. [PubMed: 15016813]
20. Rohlfs RJ, Olson JS, Gibson QH. A comparison of the geminate recombination kinetics of several monomeric heme proteins. J Biol Chem. 1988; 263:1803–1813. [PubMed: 3338995]
21. Rohlfs RJ, Mathews AJ, Carver TE, Olson JS, Springer BA, Egeberg KD, Sligar SG. The effects of amino acid substitution at position E7 (residue 64) on the kinetics of ligand binding to sperm whale myoglobin. J Biol Chem. 1990; 265:3168–3176. [PubMed: 2303446]
22. Cooper CE. Nitric oxide and iron proteins. Biochim Biophys Acta. 1999; 1411:290–309. [PubMed: 10320664]
23. Van Doorslaer S, Dewilde S, Kiger L, Nistor SV, Goovaerts E, Marden MC, Moens L. Nitric oxide binding properties of neuroglobin. A characterization by EPR and flash photolysis. J Biol Chem. 2003; 278:4919–4925. [PubMed: 12480932]
24. Fago A, Mathews AJ, Dewilde S, Moens L, Brittain T. The reactions of neuroglobin with CO: evidence for two forms of the ferrous protein. J Inorg Biochem. 2006; 100:1339–1343. [PubMed: 16684569]
25. Cassoly R, Gibson Q. Conformation, co-operativity and ligand binding in human hemoglobin. J Mol Biol. 1975; 91:301–313. [PubMed: 171411]
26. Huang Z, Shiva S, Kim-Shapiro DB, Patel RP, Ringwood LA, Irby CE, Huang KT, Ho C, Hogg N, Schechter AN, Gladwin MT. Enzymatic function of hemoglobin as a nitrite reductase that produces NO under allosteric control. J Clin Invest. 2005; 115:2099–2107. [PubMed: 16041407]
27. Azarov I, He X, Jeffers A, Basu S, Ucer B, Hantgan RR, Levy A, Kim-Shapiro DB. Rate of nitric oxide scavenging by hemoglobin bound to haptoglobin. Nitric oxide. 2008; 18:296–302. [PubMed: 18364244]
28. Azarov I, Huang KT, Basu S, Gladwin MT, Hogg N, Kim-Shapiro DB. Nitric oxide scavenging by red blood cells as a function of hematocrit and oxygenation. J Biol Chem. 2005; 280:39024–39032. [PubMed: 16186121]
29. Basu S, Azarova NA, Font MD, King SB, Hogg N, Gladwin MT, Shiva S, Kim-Shapiro DB. Nitrite reductase activity of cytochrome c. J Biol Chem. 2008; 283:32590–32597. [PubMed: 18820338]

30. Kim-Shapiro DB, King SB, Huang Z, Louderback JG, Azizi F, Goyal M. Quantification of HbNO formation upon NO addition to oxyhemoglobin under physiological conditions. Blood. 2001; 98:16b–16b.
31. Kraut JA, Madias NE. Lactic acidosis. N Engl J Med. 2014; 371:2309–2319. [PubMed: 25494270]
32. Bosch X, Poch E, Grau JM. Rhabdomyolysis and acute kidney injury. N Engl J Med. 2009; 361:62–72. [PubMed: 19571284]
33. Zinkham WH, Houtchens RA, Caughey WS. Carboxyhemoglobin levels in an unstable hemoglobin disorder (Hb Zurich): effect on phenotypic expression. Science. 1980; 209:406–408. [PubMed: 7384813]
34. Winter PM, Miller JN. Carbon monoxide poisoning. JAMA-J Am Med Assoc. 1976; 236:1502–1504.
35. Ernst A, Zibrak JD. Current concepts - Carbon monoxide poisoning. N Engl J Med. 1998; 339:1603–1608. [PubMed: 9828249]
36. Weaver LK, Howe S, Hopkins R, Chan KJ. Carboxyhemoglobin half-life in carbon monoxide-poisoned patients treated with 100% oxygen at atmospheric pressure. Chest. 2000; 117:801–808. [PubMed: 10713010]
37. Hampson NB, Hauff NM. Risk factors for short-term mortality from carbon monoxide poisoning treated with hyperbaric oxygen. Crit care med. 2008; 36:2523–2527. [PubMed: 18679118]
38. Hopkins RO, Weaver LK. Cognitive outcomes 6 years after acute carbon monoxide poisoning [abstract]. Undersea Hyperb Med. 2008:258.
39. Mimura K, Harada M, Sumiyoshi S, Tohya G, Takagi M, Fujita E, Takata A, Tatetsu S. Long-term follow-up study on sequelae of carbon monoxide poisoning; serial investigation 33 years after poisoning. Seishin Shinkeigaku Zasshi. 1999; 101:592–618. [PubMed: 10502996]
40. Weaver LK. Clinical practice. Carbon monoxide poisoning. N Engl J Med. 2009; 360:1217–1225. [PubMed: 19297574]
41. Weaver HR, Churchill LK, Deru SKK. Neurological outcomes 6 years after acute carbon monoxide poisoning [abstract]. Undersea Hyperb Med. 2008:258–259.
42. Gould SA, Moore EE, Moore FA, Haenel JB, Burch JM, Sehgal H, Sehgal L, DeWoskin R, Moss GS. Clinical utility of human polymerized hemoglobin as a blood substitute after acute trauma and urgent surgery. J Trauma-Injury Infect Crit Care. 1997; 43:325–331.
43. Noveck RJ, Shannon EJ, Leese PT, Shorr JS, Flaim KE, Keipert PE, Woods CM. Randomized safety studies of intravenous perflubron emulsion. II. Effects on immune function in healthy volunteers. Anesth Analg. 2000; 91:812–822. [PubMed: 11004031]
44. Olofsson C, Nygards EB, Ponzer S, Fagrell B, Przybelski R, Keipert PE, Winslow N, Winslow RM. A randomized, single-blind, increasing dose safety trial of an oxygen-carrying plasma expander (Hemospan (R)) administered to orthopaedic surgery patients with spinal anaesthesia. Transfus Med. 2008; 18:28–39. [PubMed: 18279190]
45. Zazzeron L, Liu C, Franco W, Nakagawa A, Farinelli WA, Bloch DB, Anderson RR, Zapol WM. Pulmonary Phototherapy for Treating Carbon Monoxide Poisoning. Am J Respir Crit Care Med. 2015; 192:1191–1199. [PubMed: 26214119]
46. Roderique JD, Josef CS, Newcomb AH, Reynolds PS, Somera LG, Spiess BD. Preclinical evaluation of injectable reduced hydroxocobalamin as an antidote to acute carbon monoxide poisoning. J Trauma Acute Care Surg. 2015; 79:S116–120. [PubMed: 26406423]
47. Kitagishi H, Negi S, Kiriyama A, Honbo A, Sugiura Y, Kawaguchi AT, Kano K. A diatomic molecule receptor that removes CO in a living organism. Angew Chem Int Ed Engl. 2010; 49:1312–1315. [PubMed: 20069620]
48. Goldbaum LR, Orellano T, Dergal E. Mechanism of the toxic action of carbon monoxide. Ann Clin Lab Sci. 1976; 6:372–376. [PubMed: 962299]
49. Brown SD, Piantadosi CA. In vivo binding of carbon monoxide to cytochrome c oxidase in rat brain. J Appl Phys. 1990; 68:604–610.
50. Brown SD, Piantadosi CA. Recovery of energy metabolism in rat brain after carbon monoxide hypoxia. J Clin Invest. 1992; 89:666–672. [PubMed: 1737854]

51. Doherty DH, Doyle MP, Curry SR, Vali RJ, Fattor TJ, Olson JS, Lemon DD. Rate of reaction with nitric oxide determines the hypertensive effect of cell-free hemoglobin. Nat Biotechnol. 1998; 16:672–676. [PubMed: 9661203]
52. Alayash AI. Blood substitutes: why haven't we been more successful? Trends Biotechnol. 2014; 32:177–185. [PubMed: 24630491]
53. Huang Z, Louderback JG, Goyal M, Azizi F, King SB, Kim-Shapiro DB. Nitric oxide binding to oxygenated hemoglobin under physiological conditions. Bba-Gen Subjects. 2001; 1568:252–260.
54. Alayash AI. Oxygen therapeutics: can we tame haemoglobin? Nat Rev Drug Discov. 2004; 3:152–159. [PubMed: 15043006]
55. Wang X, Tanus-Santos JE, Reiter CD, Dejam A, Shiva S, Smith RD, Hogg N, Gladwin MT. Biological activity of nitric oxide in the plasmatic compartment. Proc Natl Acad Sci U S A. 2004; 101:11477–11482. [PubMed: 15258287]
56. Vajpayee, GS.; Bem, NS. Basic Examination of Blood and Bone Marrow. In: McPherson, PM.; RA, editors. Henry's Clinical Diagnosis and Management by Laboratory Methods. 22. Vol. Chap 30. Saunders, an imprint of Elsevier Inc; Philadelphia, PA: 2011. p. 509-535.
57. Studier FW. Protein production by auto-induction in high-density shaking cultures. Protein Expr Purif. 2005; 41:207–234. [PubMed: 15915565]
58. Mu J, Li L, Guo Y, Qiu Z, Tan X. Spectroscopic study on acid-induced unfolding and refolding of apo-neuroglobin. Spectrochim Acta A Mol Biomol Spectrosc. 2010; 75:1600–1604. [PubMed: 20227336]
59. Edelhoch H. Spectroscopic determination of tryptophan and tyrosine in proteins. Biochemistry. 1967; 6:1948–1954. [PubMed: 6049437]
60. Hofrichter SJ, Henry JER, Eaton WA. Nanosecond absorption spectroscopy of hemoglobin: elementary processes in kinetic cooperativity. Proc Natl Acad Sci USA. 1983; 80:2235–2239. [PubMed: 6572974]
61. Birukou I, Schweers RL, Olson JS. Distal histidine stabilizes bound O2 and acts as a gate for ligand entry in both subunits of adult human hemoglobin. J Biol Chem. 2010; 285:8840–8854. [PubMed: 20080971]
62. Zijlstra WG, Vankampen EJ. Standardization of Hemoglobinometry .1. The extinction coefficient of Hemiglobincyanide at λ = 540 mμ ε^{540}_{HiCN}. Clin Chim Acta. 1960; 5:719–726. [PubMed: 13788465]
63. Schwede T, Kopp J, Guex N, Peitsch MC. SWISS-MODEL: An automated protein homology-modeling server. Nucleic Acids Res. 2003; 31:3381–3385. [PubMed: 12824332]
64. Pesce A, Dewilde S, Nardini M, Moens L, Ascenzi P, Hankeln T, Burmester T, Bolognesi M. Human brain neuroglobin structure reveals a distinct mode of controlling oxygen affinity. Structure. 2003; 11:1087–1095. [PubMed: 12962627]
65. DeLano, WL. The PyMOL molecular graphics system. 2002.
66. Vallone B, Nienhaus K, Matthes A, Brunori M, Nienhaus GU. The structure of carbonmonoxy neuroglobin reveals a heme-sliding mechanism for control of ligand affinity. Proc Natl Acad Sci U S A. 2004; 101:17351–17356. [PubMed: 15548613]
67. Polotsky VY, Rubin AE, Balbir A, Dean T, Smith PL, Schwartz AR, O'Donnell CP. Intermittent hypoxia causes REM sleep deficits and decreases EEG delta power in NREM sleep in the C57BL/6J mouse. Sleep Med. 2006; 7:7–16. [PubMed: 16309961]
68. Brantley RE Jr, Smerdon SJ, Wilkinson AJ, Singleton EW, Olson JS. The mechanism of autooxidation of myoglobin. J Biol Chem. 1993; 268:6995–7010. [PubMed: 8463233]
69. Kano K, Kitagishi H. HemoCD as an artificial oxygen carrier: oxygen binding and autoxidation. Artif Organs. 2009; 33:177–182. [PubMed: 19178464]
70. Mendes P. GEPASI: a software package for modelling the dynamics, steady states and control of biochemical and other systems. Comput Appl Biosci. 1993; 9:563–571. [PubMed: 8293329]
71. Parkhurst L. Hemoglobin and myoglobin ligand kinetics. Annu Rev Phys Chem. 1979; 30:503–546.

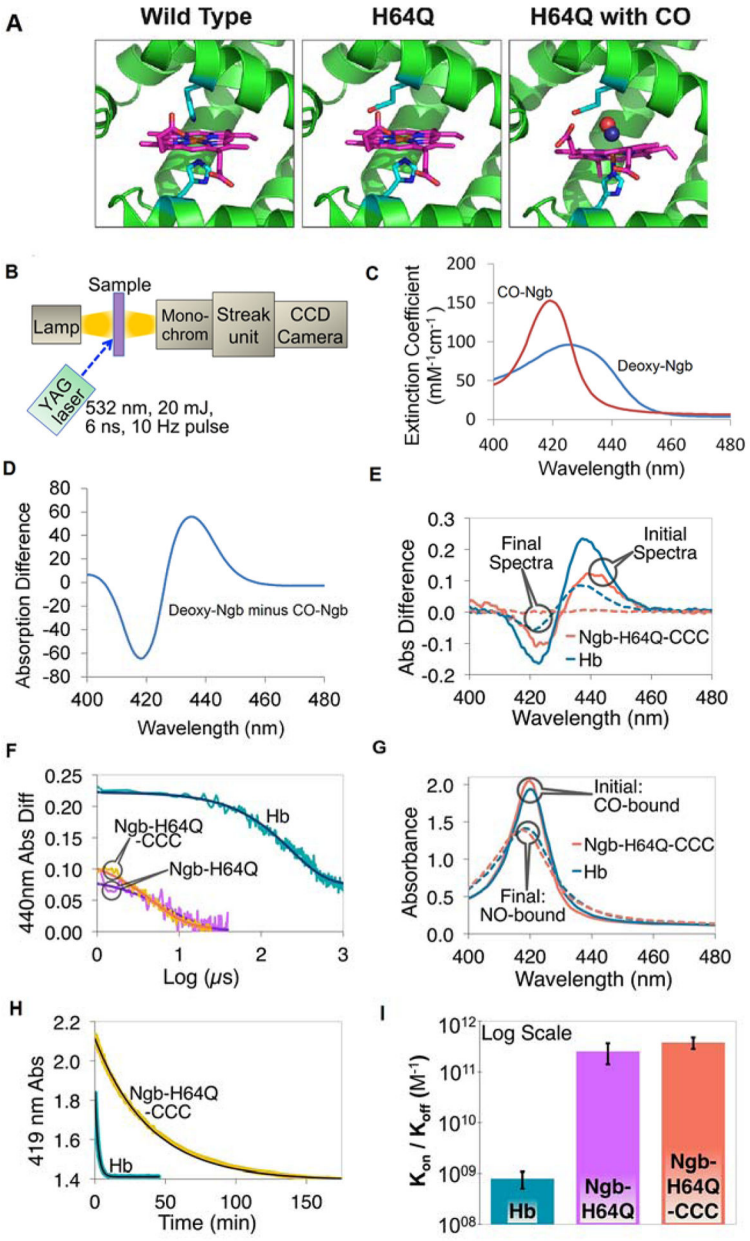

Fig. 1. Kinetics of association and dissociation of CO with hemoglobin and H64Q mutant neuroglobins

(**A**) Structure of wild-type Ngb and Ngb-H64Q mutant unliganded and with bound CO. Models for Ngb-H64Q and Ngb-H64Q-CO were built using available Ngb wild-type structures as described in Methods. **(B)** Flash Photolysis: A laser pulse dissociates CO from the heme. A mercury lamp is used to probe absorption. Light passes through the sample and then is diffracted onto a steak camera so that transmitted light is collected as a function of wavelength and time. For CO recombination kinetics were recorded for 1200 μs, 100 μs, and 50 μs for hemoglobin, Ngb-H64Q, and Ngb-H64Q-CCC, respectively (**C**) Static absorption spectra of Ngb-H64Q-CCC. Spectra were normalized by concentrations to produce extinction coefficients. (**D**) Difference spectrum of deoxy-Ngb-H64Q-CCC minus CO-Ngb-

H64Q-CCC. (**E**) Flash Photolysis: Difference between absorbance immediately after photolysis (unliganded protein) and absorbance of CO-protein ("Initial Spectra") and between absorbance of Ngb-H64Q-CCC 100 μs, or Hb 1200 μs, after photolysis and that of CO-Ngb-H64Q-CCC or CO-Hb ("Final Spectra"). Note: Hb reaction is incomplete after 1000 μs. (**F**) Flash Photolysis: Kinetics (raw data and fits) of CO binding to the globins on a logarithmic scale, with 1 mM of excess CO (k_{Hb} = 4.62 ms^{-1}; $k_{Ngb\text{-}H64Q}$ = 139 ms^{-1}; $k_{Ngb\text{-}H64Q\text{-}CCC}$ = 188 ms^{-1}) (**G**) Replacement by NO: Soret band of initial (CO-bound) and final (NO-bound) species for both Hb and Ngb-H64Q-CCC after the addition of 1 mM NO solution. (**H**) Replacement by NO: Kinetics (raw data and fits) of CO dissociation from Hb and Ngb-H64Q-CCC in presence of 1 mM excess NO (k_{Hb} = 7.65×10^{-3} s^{-1}; $k_{Ngb\text{-}H64Q\text{-}CCC}$ = 4.27×10^{-4} s^{-1}) (**I**) The overall affinity was found to be $7.95 \pm 2.87 \times 10^{8}$ M^{-1} for Hb and $2.54 \pm 1.13 \times 10^{11}$ M^{-1} and $3.80 \pm 0.96 \times 10^{11}$ M^{-1} for Ngb-H64Q and Ngb-H64Q-CCC, respectively. Error bars show SEM. All the experiments were repeated at least three times.

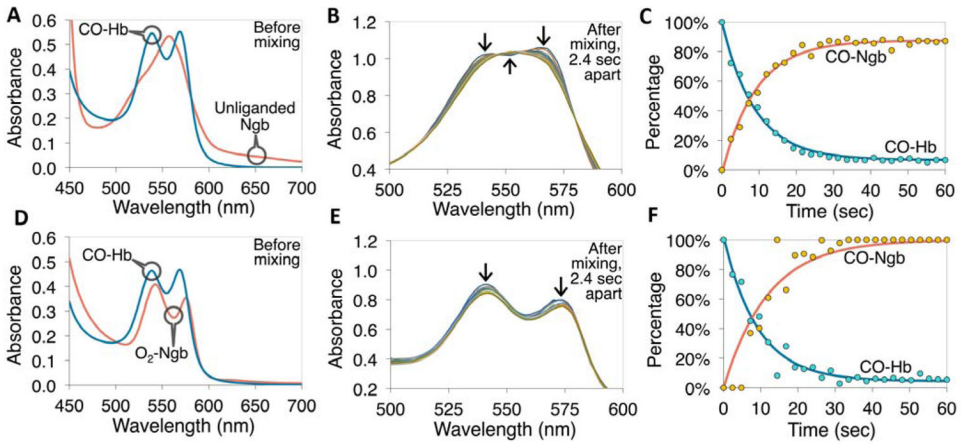

Fig. 2. CO transfer from free hemoglobin to Ngb-H64Q-CCC under anaerobic (A–C) and aerobic (D–F) conditions

(**A**) Example absorption spectra of 40 μM CO-Hb and deoxy-Ngb-H64Q-CCC before mixing the two together at 37 °C, in presence of 5 mM sodium dithionite. (**B**) Spectra measured every 2.4 s after mixing the two proteins together, arrows indicate the change in absorbance at specific wavelengths. (**C**) Kinetics (deconvoluted data and exponential fits) of the CO-Hb and CO-Ngb-H64Q-CCC species. The measured reaction rate constant was 0.11 s^{-1} (half-life 6.4 s). (**D**) Example absorption spectra of 33 μM CO-Hb and 30 μM oxy-Ngb-H64Q-CCC before mixing the two together at 37 °C, in presence of atmospheric oxygen. (**E**) Spectra measured every 2.4 s after mixing the two proteins together; arrows indicate the change in absorbance at specific wavelengths. (**F**) Kinetics (deconvoluted data and exponential fits) of the CO-Hb and CO-Ngb-H64Q-CCC species under aerobic conditions. The measured rate constant was 0.11 s^{-1} (half-life 6.4 s, equal to example in the absence of oxygen). Reference spectra are shown in Fig. S5. All the experiments were repeated at least three times.

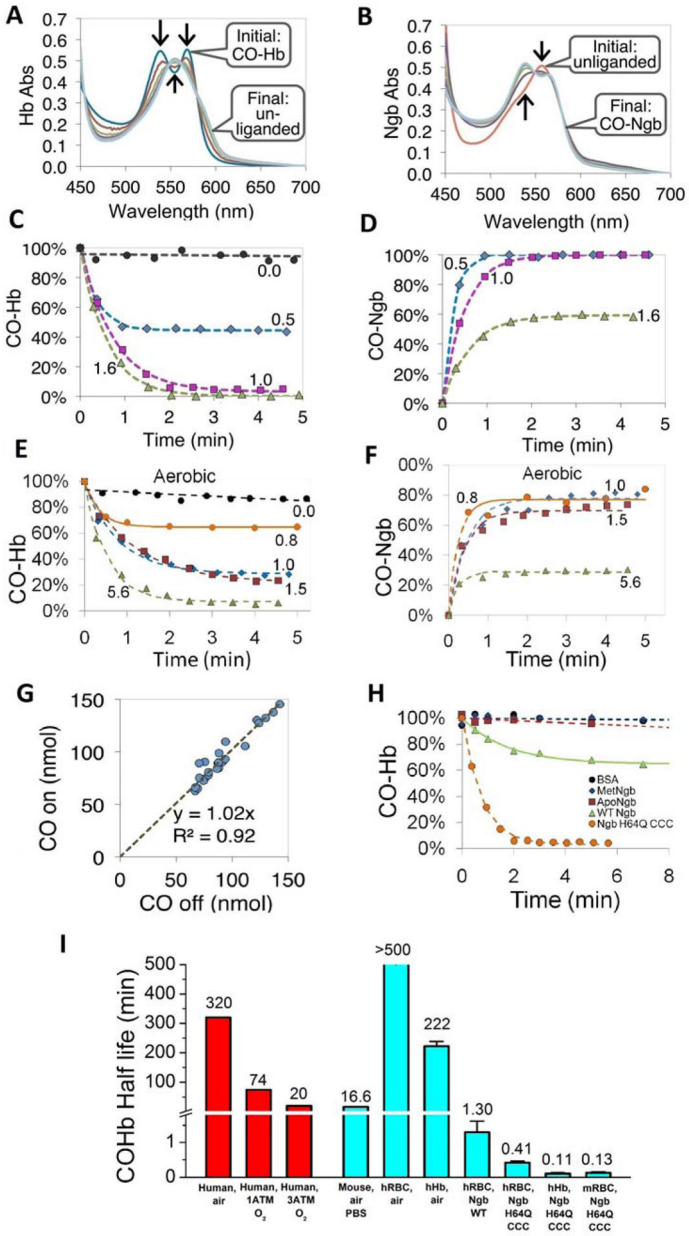

Fig. 3. CO transfer from RBC-encapsulated hemoglobin to Ngb-H64Q-CCC

(**A – B**) Absorbance spectra of 40 μM Hb and 40 μM Ngb-H64Q-CCC, respectively, after mixing CO-Hb with deoxy-Ngb-H64Q-CCC at 37 °C in presence of 10 mM sodium dithionite. Arrows indicate the direction of absorbance changes. Initial spectra were recorded before mixing. (**C – D**) Time course of CO-Hb (C) and CO--Ngb-H64Q-CCC (D) concentrations after mixing at 37 °C, in the presence of 3 – 10 mM sodium dithionite. Numbers indicate the ratio of Ngb-H64Q-CCC to Hb. The time courses for equimolar amounts of Hb and Ngb were derived from the spectra shown in (A) and (B) respectively. (**E – F**). Time course of CO-Hb (**E**) and CO--Ngb-H64Q-CCC (**F**) under aerobic conditions at 37 °C. (**G**) The calculated moles of CO dissociated from Hb (x-axis) plotted against the calculated moles of CO bound to Ngb-H64Q-CCC, based on data in **C – F**, Fig. 2 and

replicate experiments (n = 29). (**H**) Kinetic changes of RBC-encapsulated CO-Hb when mixed with BSA, met-Ngb-H64Q-CCC, apo-Ngb-H64Q-CCC, wild type Ngb and deoxy Ngb-H64Q-CCC, Protein:Hb ratios used were 2 for BSA and 1 for met-Ngb, ApoNgb, WtNgb and deoxy Ngb-H64Q-CCC. (**I**) Half-lives of CO dissociation from RBC-encapsulated or free Hb in mice and human. Human *in vivo* values were obtained from the literature (1, 34, 36). Other values were measured in this work. Error bars show SEM. The experiments were repeated at least three times.

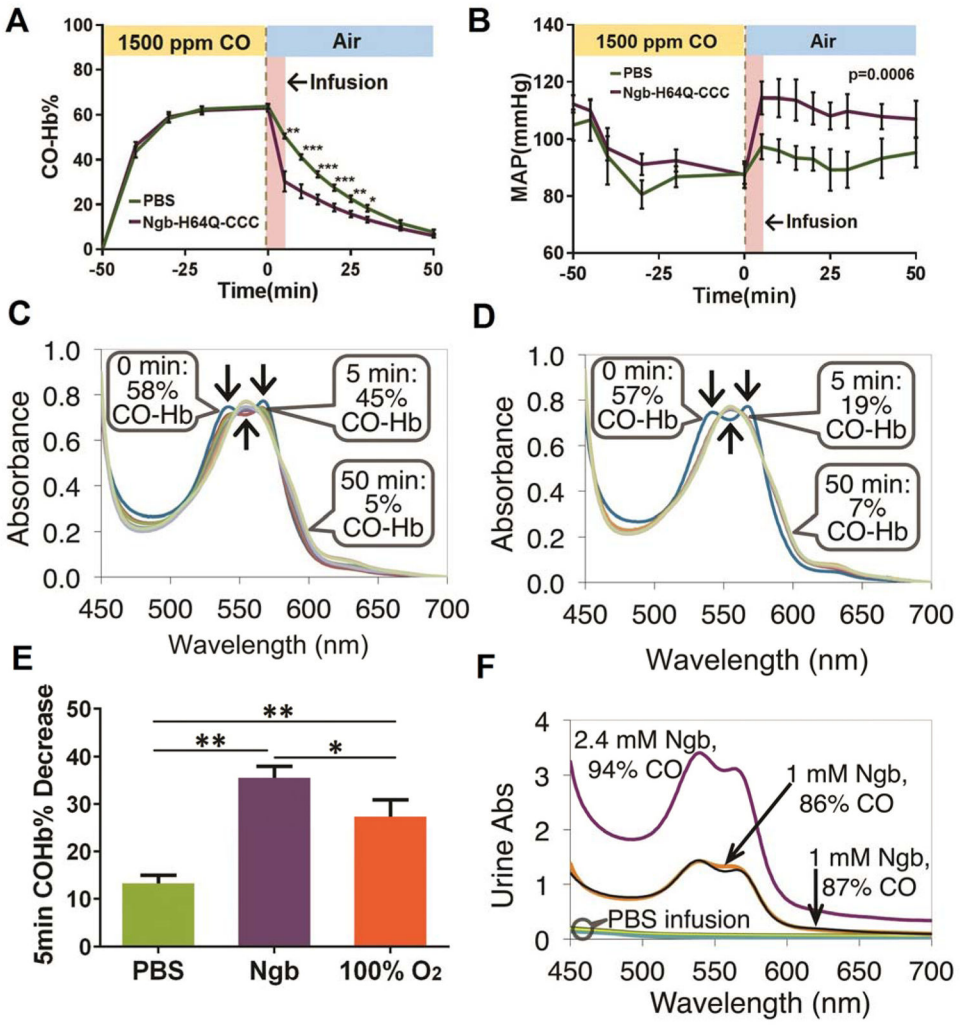

Fig. 4. In vivo CO transfer from RBC-encapsulated hemoglobin to Ngb-H64Q-CCC

(A – B) Time course of RBC-encapsulated CO-Hb (**A**) and mean arterial pressure (MAP)(**B**) before and after exposure of mice to CO. Mice were exposed to 1500 ppm of CO for 50 minutes; then (x = 0 min) CO was turned off and animals returned to normal atmospheric conditions. At the same time, 250 μL of either PBS or Ngb-H64Q-CCC (9 – 12 mM) were infused within 4 minutes. RBC-encapsulated CO-Hb and MAP were periodically measured before and after treatment. Data are expressed as mean ± SEM and * $P < 0.05$, ** $P < 0.01$, *** $P < 0.005$ were calculated with the 2-tail unequal variances Student's t-test. $P = 0.0006$ for MAP for time > 0, from mixed effect model with unstructured covariance. (**C – D)** Absorbance spectra of mouse Hb from representative experiments with PBS (C) or Ngb-H64Q-CCC infusion (D). The spectra correspond to the time points in (A)0 and (B). (**E**) Decrease in CO-Hb% 5 minutes after end of CO exposure for mice that received PBS (n = 7), Ngb-H64Q-CCC (n = 6) or 100% oxygen inhalation (n = 5). Error bars show SEM. *P*-values were calculated by one way ANOVA. *$P < 0.05$, ** $P < 0.01$. (**F**) Absorbance of urine collected after the mice were sacrificed, 60 minutes after the end of CO exposure. Three mice that received Ngb-H64Q-CCC had a high CO-Ngb urine content, while urine from the mice that received PBS did not contain heme proteins.

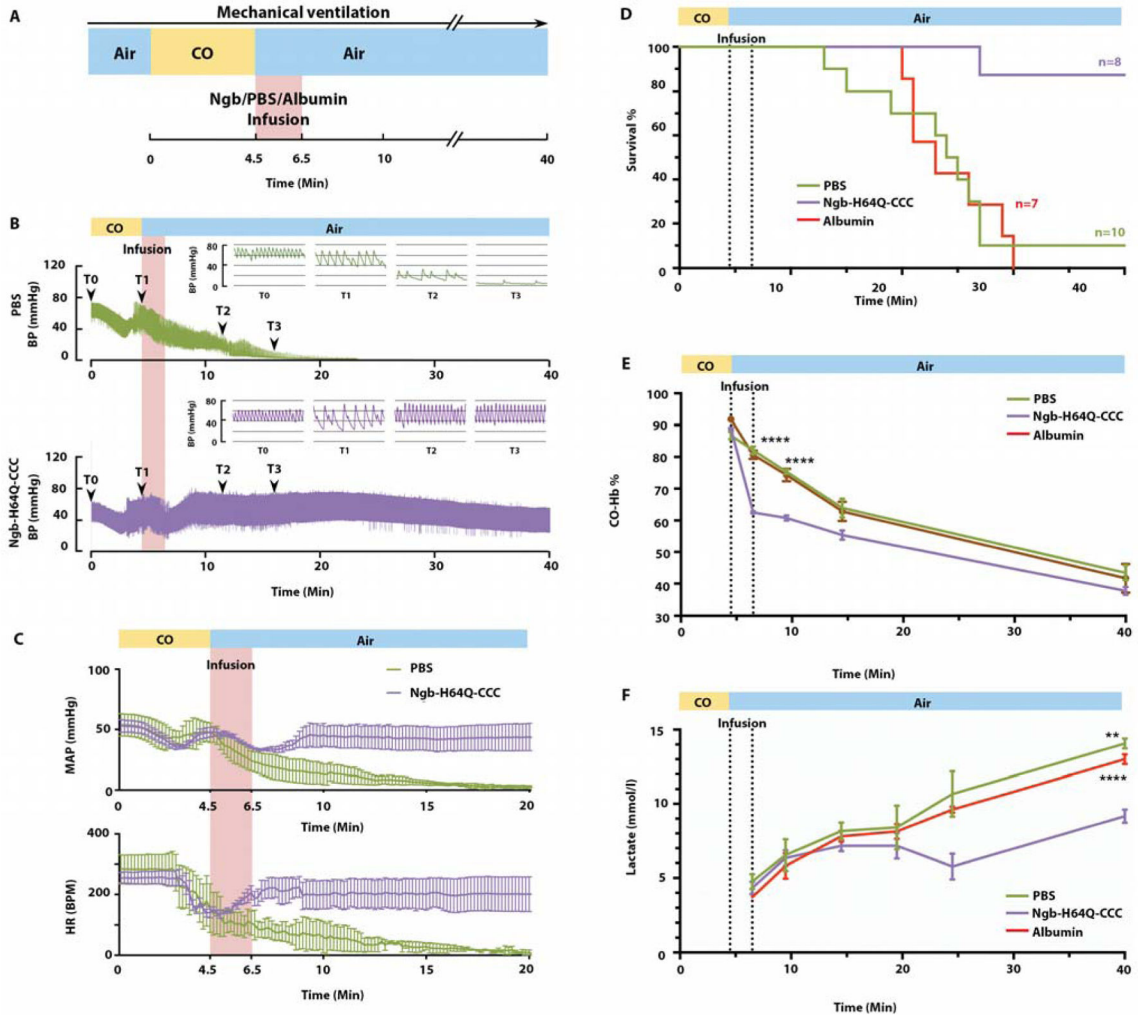

Fig. 5. Ngb-H64Q-CCC increases survival rate in a lethal CO poisoning model

(**A**) Experimental scheme of the lethal CO poisoning model. Ventilation was initiated after the surgery with a volume controlled ventilator. 3% CO mixed with air was delivered for 4.5 minutes via the ventilator. Air was delivered after stopping CO exposure and the Ngb-H64Q-CCC or PBS/albumin control was infused within 2 minutes. All mice were followed for a pre-defined experimental observation period of 40-minutes. (**B**) Mean arterial blood pressure (MAP) and heart rate (HR) changes in mice treated with PBS and Ngb-H64Q-CCC. All data are expressed as means ± SEM. (**C**) Representative MAP changes in one mouse treated with PBS and one Ngb-H64Q-CCC treated survivor. (**D**) Kaplan-Meier survival curves of mice exposed to 3% CO for 4.5min treated with PBS only ($n = 10$), albumin 5mM (n = 7) or Ngb-H64Q-CCC ($n = 8$) (Log-rank test survival, $P = 0.0008$). (E) Time course of RBC-encapsulated CO-Hb with Ngb-H64Q-CCC (n = 3) vs. PBS (n = 4) and albumin (n=4) in lethal CO poisoning model. Data are expressed as mean ± SEM, $P < 0.0001$. (**F**) Lactate level elevation is lessened with Ngb-H64Q-CCC treatment (n = 3) vs. PBS (n = 4) and albumin (n = 4) in lethal CO poisoning.

Table 1

Binding parameters for oxygen and carbon monoxide of hemoglobin and neuroglobin

Protein	O_2 k_{on} ($M^{-1}s^{-1}$)	O_2 k_{off} (s^{-1})	O_2 K_A (M^{-1})	CO k_{on} ($M^{-1}s^{-1}$)	CO k_{off} (s^{-1})	CO K_A (M^{-1})	M (K_ACO/K_AO_2)	k_{autox} (h^{-1})
Hb R [a]	5.0×10^7	1.5×10^1	3.3×10^6	6.0×10^6	1.0×10^{-2}	6.0×10^8	1.8×10^2	*ND*
Hb T [a]	4.5×10^6	1.9×10^3	2.4×10^3	8.3×10^4	9.0×10^{-2}	9.2×10^5	3.9×10^2	*ND*
hNgb [b]	2.5×10^8	0.8	3.1×10^8	6.5×10^7	1.4×10^{-2}	4.6×10^8	14	5.4
hNgb H64Q-CCC [c]	7.2×10^8	18	3.9×10^7	1.6×10^8	4.2×10^{-4}	3.8×10^{11}	9.7×10^3	0.83

[a](22);

[b](14);

[c]This work.

ND, not determined